Tab 1

Investigating the Expression of the Gene *Dronc* in *Drosophila melanogaster*

by

Phoebe Grabowski

A Paper Presented to the

Faculty of Mount Holyoke College in

Partial Fulfillment of the Requirements for

the Degree of Bachelors of Arts with

Honor

Department of Biological Sciences

South Hadley, MA 01075

May 2026

This paper was prepared

under the direction of

Professor Craig Woodard

for eight credits.

Dedicated to the memory of my grandmother,

the biologist Sharon McClure.

ACKNOWLEDGEMENTS

First, I would like to thank Professor Craig Woodard for introducing me to his lab, and for his mentorship and guidance during this research. Performing research in the Woodard Lab has been an incredible opportunity, and has given me the confidence and experience I need to further pursue the sciences. These two and a half years in the Woodard Lab have been the best part of my Mount Holyoke experience. I will forever be grateful for your support, guidance, and patience, which have made me the scientist I am today.

Secondly, I would like to thank the Mount Holyoke College Biological Sciences department for both the opportunity and means to pursue this research.

I would also like to thank the other members of my thesis advisory committee, Douglas Roosien and Scott Bassler, for their support and insight. Your assistance with the technical and professional aspects of my research mean the world to me.

Another person deserving of thanks is Professor Ishfaaq Mohammed Imtiyas, for his assistance with statistical analysis and ANOVA tests. I would also like to thank all of the people who helped me along this journey. That includes members of the Woodard Lab both past and present, such as Shweta Kiran-Cavale and Anna Narin. Another thanks is necessary for the people that helped me become the writer I am today, including Dr. Daniel Brooks, my mother Molly Grabowski, and my dear friend CJ.

Finally, I want to thank my younger sister, Celeste Grabowski. Her childhood food allergies resulted in me being well-versed in cross-contamination. That understanding is what led me to devise my hypothesis for this experiment, where I'm concerned about which cells have had contact with a hormone and for how long. Life-threatening food allergies can make your world seem so small, and I'd never have imagined that this experience would open so many doors. Celeste- I love you. Thank you.

TABLE OF CONTENTS

LIST OF FIGURES

LIST OF TABLES

ABSTRACT

Programmed Cell Death (PCD) is the process whereby cells undergo self-destruction for development or maintenance of homeostasis. Apoptosis, a form of PCD, is highly regulated by a series of molecular signals. In *Drosophila melanogaster* the steroid hormone 20-hydroxyecdysone (ecdysone) controls tissue development and metamorphosis (Bond et al., 2010; Yamanaka et al., 2013). My goal was to explore the role of ecdysone in PCD. A pulse of ecdysone occurs at 10 hours after puparium formation (APF), inducing the prepupal-pupal transition (Lee et al., 2002). In response to this ecdysone pulse, salivary gland cells undergo apoptosis (Lee et al., 2002). At the same time, ecdysone induces dissociation of fat body cells (Bond et al., 2011). It is my goal to add to the dataset of Cavale (2023), by comparing *Dronc* in the same tissues: salivary glands (experimental) and the fat body (control). Due to the spatiotemporal spread of ecdysone, anterior and posterior sections of the fat body were analyzed separately.

Gene expression was quantified by RT-qPCR, and when possible, a standard curve was included to account for individual primer efficiencies. Two-way ANOVA analysis showed no significant difference between the *Dronc* expression at 10 and 12 hrs. APF ($p=0.142$), nor in the *Dronc* expression between anterior and posterior fat body cells ($p=0.186$). There was also no significant evidence that the positioning of the fat body (anterior or posterior) influenced *Dronc* expression ($p=0.571$) at the two timepoints. To further investigate the anterior/posterior differences, the *Dronc* expression of each anterior sample was divided by its posterior counterpart. Assuming no difference, the ratio should be 1. A one-sided t-test showed significant difference between the observed and theoretical anterior/posterior ratio of 1 at 10 hrs. APF ($p=0.043$), but the difference was insignificant at 12 hrs. APF ($p=0.197$).

INTRODUCTION

I. Programmed Cell Death

Apoptosis

Programmed Cell Death (PCD) is the process wherein a cell 'self-destructs' in response to a series of signals. PCD can be used to eliminate unhealthy or unneeded cells in the organism, and therefore plays a key role in regulating homeostasis. There are three main forms of PCD: apoptosis, autophagy, and necrosis, known respectively as PCD Types I, II, and III (Ouyang et al., 2012). Necrosis is an uncontrolled form of cell death, incited by injury to the cell, which results in swelling, DNA fragmentation, and local inflammation (Khalid & Azimpouran, 2025). This process is passive, and defined by lacking characteristics of Type I and II PCD. Autophagy (Type II PCD) begins with the formation of autophagosomes, which then consume the cell's components for recycling. This can be beneficial for low-energy environments, such as starvation.

Apoptosis (Type I PCD) occurs normally during aging and development, both for disposal of unwanted or unneeded cells, but also as a form of remodeling. In *Drosophila melanogaster,* apoptosis is one mechanism utilized during morphogenesis to remodel tissues. Apoptosis is morphologically distinct from other kinds of cell death (Shen et al., 2023). It is characterised by small clusters of cells shrinking and undergoing chromatin condensation (Elmore, 2007). The cells then undergo 'budding', a process wherein apoptotic bodies are extruded from the

cell. Apoptotic bodies are membrane-bound cell fragments containing cytosol, organelles, and sometimes nuclear fragments. These apoptotic bodies leave the cell, and then are digested by macrophages for recycling of the components. One of the traits distinguishing apoptosis from necrosis is that when a cell undergoes apoptosis, nearby cells are not inflamed or damaged. Because the apoptotic mechanisms are highly conserved, apoptosis can be easily studied in model organisms, though some triggers vary between species.

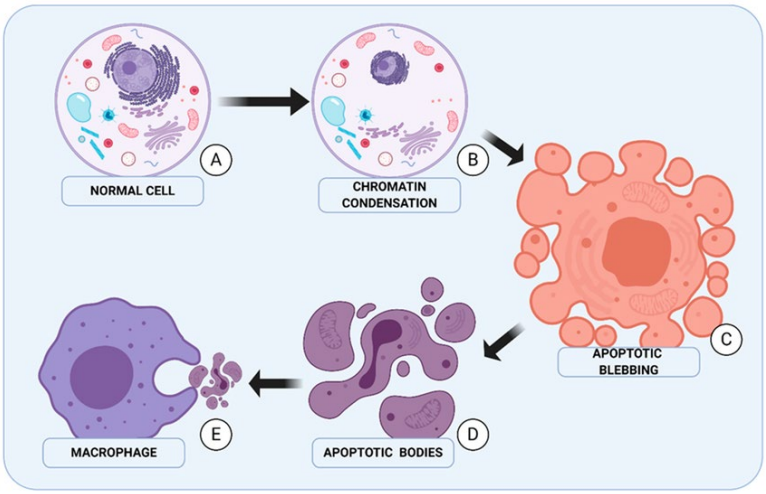

Figure 1. Phases of apoptosis. A normal cell receives apoptotic signals, after which the chromatin condenses, followed by membrane blebbing and the formation of apoptotic bodies. Once broken into small enough pieces, they can be consumed by a macrophage (Chmurska et al., 2021).

Apoptosis plays a key role in regulation of homeostasis (Elmore, 2007). Both the nervous and immune systems develop through overproduction of cells. By utilizing apoptosis, cells which fail to adopt the necessary traits are eliminated. Apoptosis also plays a role in the healing of wounds, by removing inflammatory cells. Yet another function of apoptosis is the prevention of cancer and oncogenes

(Lopez & Tait, 2015). Apoptosis is the most commonly deregulated variant of malignant cell death. It is so vital to the function of an organism that in order for cancerous cells to proliferate, it is necessary to inhibit apoptosis.

Despite its benefits for the organism, when apoptosis goes uncontrolled it can lead to disastrous consequences. Alzheimer's Disease is associated with uncontrolled neuronal apoptosis, which affects all regions of the brain responsible for symptoms of Alzheimer's (Sharma et al., 2021). Neuronal death starts slowly in the disease's early stages, and progresses with the growing strength of symptoms. While apoptosis is not the cause of Alzheimer's Disease, and it cannot fully explain the disease's pathways, it is the primary cause of the neurological symptoms. In this disease, the initiation of apoptosis via caspases is associated with increased production of the amyloid-β plaques characteristic of Alzheimer's. Because apoptosis is a highly regulated mechanism, it is thought that a potential avenue of treatment for Alzheimer's Disease could be upregulation of antiapoptotic signals. This would effectively halt apoptosis, reducing symptoms and preventing further progression of the disease.

Initiation of Apoptosis

There are two primary pathways for the activation of apoptosis- the extrinsic (death receptor) pathway and the intrinsic (mitochondrial) pathway. Each pathway leads to the activation of executioner caspases. Caspases are cysteine-aspartate proteases that act as the machinery of PCD (Green, 2022b). Caspases are initially synthesized in the cell as inactive procaspases, which can be

activated by other caspases. In vertebrates there are at least two kinds of caspases: Initiator Caspases and Executioner Caspases. Initiators send 'upstream' inter-caspase signals to continue the cascade, and Executioners are the caspases which lead to cleaving of protein substrates (Anson et al., 2021). Each procaspase (the term for an unactivated caspase) contains three domains, the prodomain, the large subunit, and the small subunit (Green, 2022b). In between the large and small subunit lies the site or sites of cleavage for that particular Programmed Cell Death (PCD) is a process wherein cells and tissues undergo self-destruction for development or maintenance of homeostasis. Apoptosis, a form of PCD, is highly regulated by a series of molecular signals. I am examining the regulation of PCD by hormonal signaling. In *Drosophila melanogaster* the regulatory steroid hormone 20-hydroxyecdysone (referred to as ecdysone) controls tissue development and metamorphosis (Bond et al., 2010; Yamanaka et al., 2013). A key pulse of ecdysone occurs at 10 hours after puparium formation (APF), inducing the prepupal to pupal transition (Lee et al., 2002). In response to this ecdysone pulse, salivary gland cells undergo apoptosis (Lee et al., 2002). At this same time, fat body cells are induced to dissociate by the ecdysone pulse (Bond et al., 2011). It is the goal of this research to add to the dataset of Cavale (2023), by comparing *Dronc* in the same experimental and control tissues: salivary glands and the fat body. Due to the spatiotemporal spread of ecdysone and the motile nature of adipocytes, both anterior and posterior sections of the fat body were analyzed here.

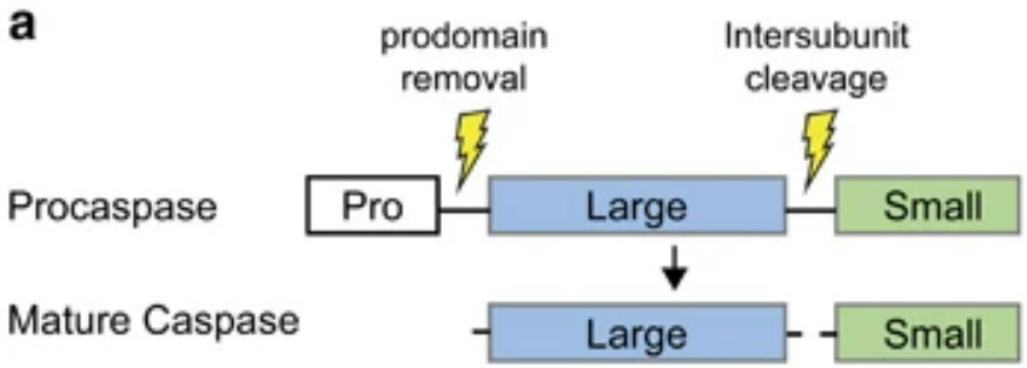

Figure 2. An uncleaved procaspase next to a mature, cleaved caspase. 'Pro' is the prodomain, 'Large' is the large subunit, and 'Small' is the small subunit (Julien & Wells, 2017).

Executioner caspases can be activated through cleavage by an initiator caspase. Activation of initiator caspases is more complex; initiator caspases exist in the cell as inactive monomers, which must be dimerized for activation (Green, 2022a). This, however, is unstable, leading to the self-cleavage of a caspase between its large and small subunits, not for activation, but rather stabilization of the active caspase. Once active, caspases are able to cleave proteins at aspartic acid residues. The activity of caspases is seen as an irreversible commitment toward death by the cell (Elmore, 2007a).

Both the intrinsic and extrinsic apoptotic pathways lead to activation of the executioner caspase-3 for initiation of apoptosis (Mustafa et al., 2024). In humans, the extrinsic pathway occurs when a death ligand binds to an extracellular death receptor, which forms a death-inducing signaling complex (DISC). The DISC is then able to activate caspase-8, an initiator caspase. This leads to activation of executor caspases, such as caspase-3, and initiates apoptosis.

The intrinsic pathway is initiated by mitochondrial response to stress, damage, or hypoxia. This causes the mitochondrial membranes to become permeable, allowing for the release of cytochrome c. Cytochrome c, now free in the cytosol, binds to and inhibits the adaptor molecule APAF-1. These structures form a complex known as the apoptosome, which recruits and activates procaspase-9. The now-active caspase-9 inhibits IAPs (Inhibitor of Apoptosis Protein), thereby allowing the cleavage and activation of executioner caspases-3 and -7. (Elmore, 2007).

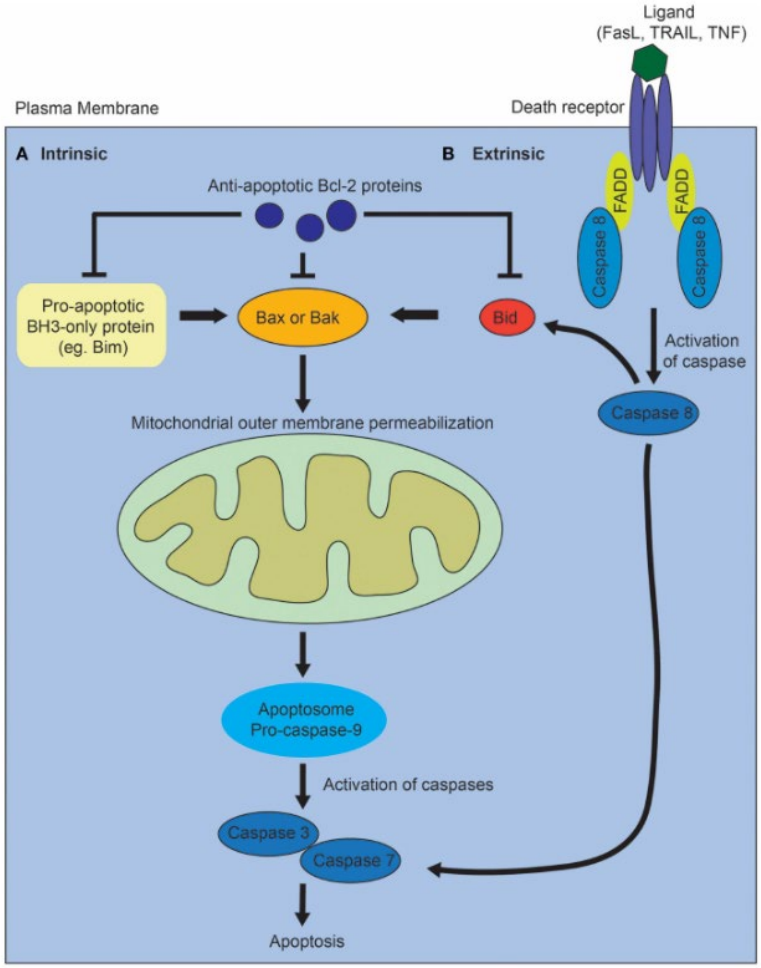

Figure 3. The intrinsic and extrinsic cell-death signalling pathways. 'A' displays the intrinsic pathway, and 'B' displays the extrinsic pathway (Ho, 2014).

II. Model Organism: *Drosophila melanogaster*

Drosophila melanogaster Life Cycle

The common fruit fly, *Drosophila melanogaster*, is a well-studied model organism for apoptosis, given that much is evolutionarily conserved between fly and human apoptotic pathways (Kornbluth & White, 2005). One of the mechanisms conserved is the use of caspases, though the individual caspases can vary in number and molecular structure between species. Additionally,

Drosophila is a relatively low-maintenance organism, with low associated costs. It takes around ten days for *Drosophila melanogaster.* to go from fertilized egg to adult (at 25°C), with a short lifespan of around 60-80 days (Fernández-Moreno et al., 2007). This short life cycle allows generational gene analysis through the lens of *Drosophila.* The life cycle can be divided into four stages: embryo, larva, pupa, and adult.

Approximately 24 hours after egg-laying, the first instar larva will emerge (Fernández-Moreno et al., 2007). Once emerged, the larva will begin feeding on the surface of the medium. This feeding is essential, because the nutrition gathered in the larval stage sustains the organism through metamorphosis (Allocca et al., 2018). Molting, the process of shedding the exoskeleton, progresses development through the instar phases, numbered by its development stage. After one molt, the now-second instar larva burrows into the medium. The second molt occurs there, resulting in the third instar larva, which will later emerge from the medium and begin crawling up the walls of the bottle. The third instar larva does this in search of a suitable place for pupariation. Once a suitable place is found, the larva undergoes a brief prepupal phase, before it develops into a pupa, a form it will remain in for around 4 days (Fernández-Moreno et al., 2007). The adult fly emerges from the pupal case (eclosion) 10-12 days after egg fertilization, and has a lifespan of 60-80 days (Basumatary & Deka, 2024; Fernández-Moreno et al., 2007). Males are immediately sexually mature, whereas it takes females 8-10 hours to reach sexual maturity after eclosion.

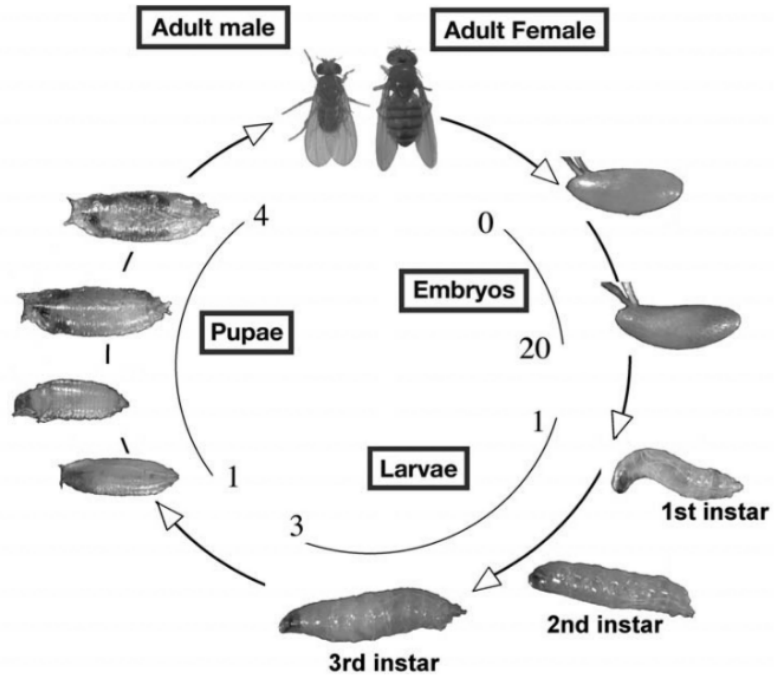

Figure 4. The *D. melanogaster* lifecycle is divided into four stages: embryo, larva, pupa, and adult. Approximate time is given in hours for embryo and larva, and in days for pupa and adult (Fernández-Moreno et al., 2007).

During the pupal phase, embryonic and larval tissues are degraded, while the imaginal discs begin to develop adult tissues. Imaginal discs are epithelial structures which develop early in the embryo, and when these discs are mature, they are triggered by the ecdysone hormonal cascade. The discs evert and differentiate, thereby giving rise to developed adult structures such as legs and wings (Beira & Paro, 2016).

III. PCD and Metamorphosis in *Drosophila*

Ecdysone Signaling

In *Drosophila melanogaster,* the regulatory steroid hormone 20-hydroxyecdysone (hereafter referred to as ecdysone), and Juvenile Hormone (JH) regulate tissue development, developmental transitions, reproduction, and metamorphosis (Bond et al., 2010; Yamanaka et al., 2013). Pulses of ecdysone during the first and second larval instar induce molting, with an increased titer of ecdysone in the late third instar triggering puparium formation and leading to metamorphosis. JH can be considered the hormone that maintains the larval stage 'status quo'. When JH is present, pulses of ecdysone will induce a larval molt, whereas in the absence of JH, an ecdysone pulse will initiate prepupal development (Jindra et al., 2013). Before pupariation, in addition to a rise in the titer of ecdysone, JH inhibition is inhibited, coupled with an increased JH metabolism. Ecdysone is produced primarily in the prothoracic gland and brought to the hemolymph to be converted into its active form (20-hydroxyecdysone), where it is then able to bind to nuclear receptors. JH is produced in the corpora allata, a pair of glands posterior to the brain.

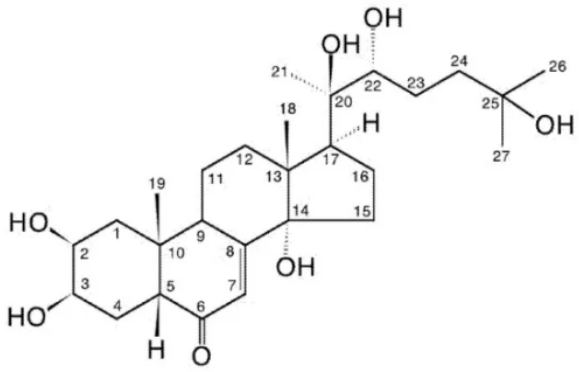

Figure 5. 20-hydroxyecdysone, the activated form of ecdysone. Inactive ecdysone lacks the 20-hydroxyl group (Lafont et al., 2021).

The ecdysone receptor is a heterodimer composed of nuclear hormone receptors encoded by *Ecdysone Receptor (EcR)* and *Ultraspiracle (USP)* (Baehrecke, 2000). Receptors bind to Hormone Response Elements (HRE) to function as transcription factors, in the case of ecdysone, an Ecdysone Response Element (EcRE) (Cherbas et al., 1991). The EcRE sequence and receptor binding suggest that these mechanisms are highly conserved, and similar to those of vertebrates.

The EcR-USP heterodimer represses the transcription of early metamorphic genes. When ecdysone binds to the EcR-USP heterodimer, this relieves the repressive activity, allowing transcription (Schubiger et al., 2005). In short, the binding of ecdysone to the EcR-USP heterodimer allows the transcription of genes necessary for *D. melanogaster* to proceed with early metamorphosis. Ecdysone plays an important role in repression and activation for the regulation of metamorphic timing. Loss of USP function in imaginal discs

results in not only failure to transcribe early genes, but also failure to repress genes which must be expressed at a later stage (precocious differentiation) (Schubiger et al., 2005). Likewise, loss of EcR function in wing discs results in premature *BR-Z1* expression as well as differentiation of the sensory neurons. In summary, the EcR-USP heterodimer binds to both ecdysone and the EcRE in order to relieve the gene repression done by EcR-USP, thereby allowing properly timed transcription of metamorphic genes.

EcR-USP binding induces expression of several genes associated with molting and metamorphosis during developmental increases in ecdysone, here referred to ecdysone pulses. There are two major ecdysone pulses concerning the early processes of morphogenesis, the late larval pulse and the prepupal pulse. The late larval ecdysone pulse provides a signal for pupariation to begin, and prepupal pulse around 10 hrs. APF results in PCD and developmental remodeling (Broadus et al., 1999). The late larval ecdysone pulse induces transcription of the genes *BR-C*, *E74A*, and *E75A*, which is followed by anterior muscle and midgut cell death (Baehrecke, 2000). The prepupal ecdysone pulse then occurs, inducing another wave of transcription of *BR-C*, *E74A*, and *E75A*, as well as induction of *E93* in the salivary glands. This results in the PCD of the salivary glands, head eversion, and further development of the adult organs. Between these pulses, the ecdysone titer decreases to a low concentration, before peaking again. This momentary decrease allows for the expression of the competence factor βFTZ-F1 (encoded by the gene, *ßFTZ-F1*), which allows further adult development.

βFTZ-F1

βFTZ-F1 is a *D. melanogaster* competence factor. A competence factor is a molecule within the cell that permits a certain developmental response, and is closely regulated. *βFTZ-F1* has no direct effect on gene expression at the onset of metamorphosis, but it assists the expression of *BR-C*, *E74A*, *E75A,* and *E93* in response to the prepupal ecdysone pulse (Woodard et al., 1994). Antibody staining (Lavorgna et al., 1993) showed that the βFTZ-F1 protein can be found bound to many ecdysone-regulated polytene chromosome puffs in salivary glands during late prepupal stages. In particular, strongly stained regions were those of genes *E74, E75,* and *E93*. *βFTZ-F1* activity is repressed in the presence of ecdysone, it is expressed during the larval and mid prepupal phases. Prepupal induction of *βFTZ-F1* is caused by the temporary decrease in ecdysone titer between the late larval and prepupal ecdysone pulses. Not only is it important for the ecdysone titer to increase, but it must also decrease at the appropriate developmental times.

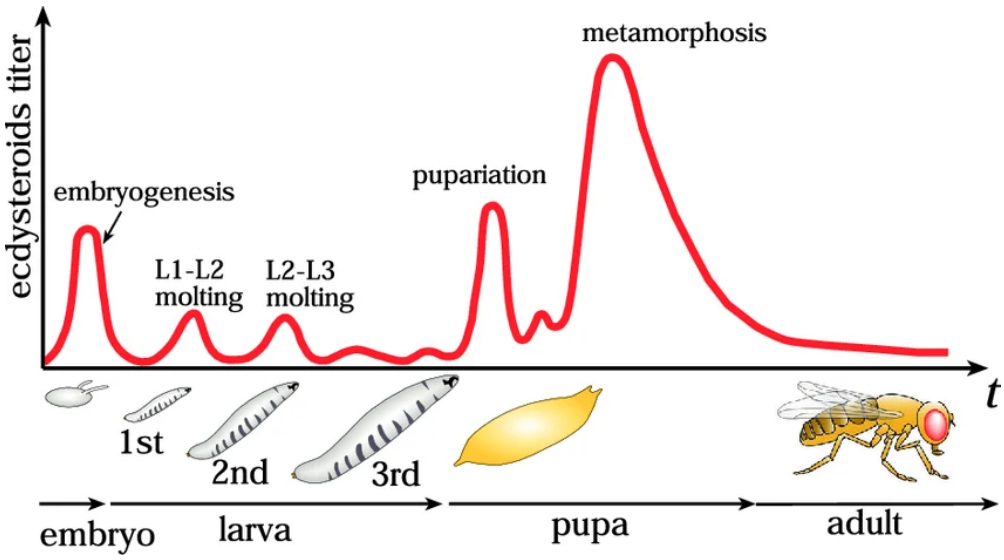

Figure 6. Ecdysteroid titer at different points during *D. melanogaster* development. The prepupal phase is indicated by the 'pupariation' pulse of ecdysone, followed by the second, smaller increase in ecdysone titer, involved in pupal development (Riddiford, 1993).

Relevance of Salivary Glands and Larval Fat Body

As *D. melanogaster* development occurs, the steroid hormone ecdysone is released and activated by conversion to 20-hydroxyecdysone (hereafter referred to simply as ecdysone). Ecdysone and the competence factor ßFTZ-F1 are necessary to determine the length of developmental stages (Bond et al., 2010). The prepupal ecdysone pulse induces several changes in the pupa.

The salivary glands are an organ composed of two secretory glands, connected by individual salivary ducts to a central common duct (Kim et al., 2026). During the third instar stage of larval development, the salivary glands synthesize and secrete 'glue' proteins. These are adhesive proteins, which the larva will use to secure the pupal case for metamorphosis. The second pulse of

ecdysone in the salivary glands during the prepupal phase induces transcription of *E93*, *E74*, and *BR-C*, which are genes responsible for caspase execution (Lee et al., 2002). This causes the apoptosis of the salivary glands cells, in order to allow for formation of adult tissues.

Ecdysone also drives apoptosis of other tissues, such as the larval midgut. The midgut condenses during late third instar larval development, shown in larvae 4 hours before puparium formation (Jiang et al., 1997). During puparium formation there is a noticeable shortening of the gastric caeca, structures which improve nutrient absorption. Between 2 and 4 hours after puparium formation, the midgut contracts, and the gastric caeca disappear. Late third instar larvae which were injected with ecdysone underwent uniform midgut cell death 8-10 hours after exposure, whereas larvae without ecdysone treatment did not. The dye used in this study, acridine orange, demonstrated that the midgut cells were destroyed via apoptosis. During larval midgut cell death, there is a high level of caspase activity. However, larval midgut cell death is able to proceed in the absence of caspases, such as *Dronc* (Denton et al., 2010). There is a greater reliance on machinery of autophagy in the destruction of the larval midgut, though its relationship to caspases is still unclear.

The fat body is an organ which serves as the equivalent to vertebrate adipose tissue and liver (Liu et al., 2009). During the larval phase, there is no increase in the number of fat body cells, although there is an increase in size as the larva feeds to store energy. At this stage, the fat body exists as a single layer

of white, tightly-associated cells. These cells gradually become spherical, and after pupariation begin to dissociate into individuals, in a process called 'remodeling' (Nelliot et al., 2006). The hormone ecdysone drives this remodelling both in the pupariation ecdysone pulse as well as the 10-12 hrs. APF pulse. In the fat body, the exposure to ecdysone and activation of *ßFTZ-F1* induces dissociation and detachment from adjacent adipocytes (Bond et al., 2011).

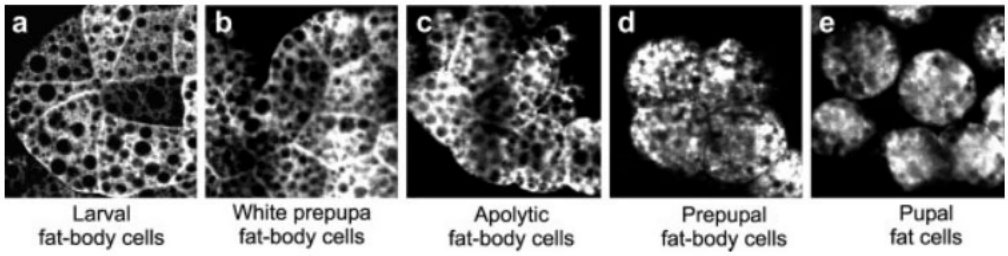

Figure 7. Fat body cell remodeling through the larval to pupal transition, with 'Apolytic' being the 6 APF prepupa, and the 'Prepupal' being between 8 and 10 hrs. APF (Nelliot et al., 2006).

In addition to providing energy for pupal development, the persistence of larval fat body cells into the adult fly provides vital nutrition for newly eclosed adults (Aguila et al., 2007). When *EcR* expression is silenced in the fat body, it leads to increased pupal size, as well as increased size at pupariation (Colombani et al., 2005). After the dissociation and remodeling of the larval fat body, the adipocytes are motile, migrating toward portions of the organism that require wound healing (Franz et al., 2018).

The human initiator caspase-9 is homologous to the *Drosophila* caspase Dronc (Hay & Guo, 2006), however, the exact role of the gene *Dronc* is poorly

understood. *Dronc* expression is associated with caspase-dependent cell death, with complex underlying mechanisms. DrICE is a downstream effector caspase required for the execution of apoptosis (Meier et al., 2000), and this caspase is activated by proteins HID (Head Involution Defective), RPR (Reaper), GRIM. HID, RPR, and GRIM require activation by *E93.* DrICE is also activated by Dronc, though through a less clearly defined pathway. *Drosophila* Inhibitor of Apoptosis Protein 1 (DIAP1) represses Dronc and DrICE caspase activity through interaction with the Dronc prodomain. Some studies have shown *Dronc* expression to be critical for salivary gland histolysis (Daish et al., 2004).

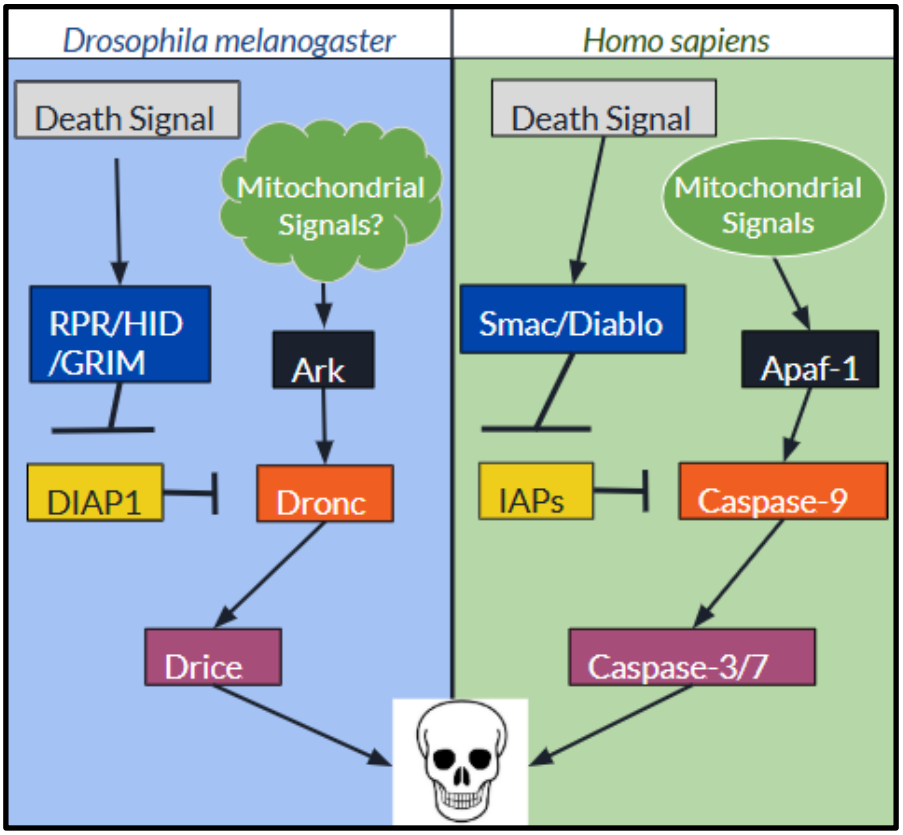

Figure 8. The *Drosophila melanogaster* caspase pathway toward initiation of apoptosis, alongside *Homo sapiens* orthologs of each protein in the pathway. The outcome of the pathway, apoptosis, is represented by the skull. The role of mitochondrial signals in activating Ark is still poorly understood, which is why that step in the *D. melanogaster* pathway has a question mark attached.

In order to study the caspase Dronc, the salivary glands will be used as the experimental tissue due to the regulated PCD that occurs after the 10-12 hrs. APF ecdysone pulse. The control tissue, the fat body, was selected due to its regulated nonlethal reaction to the same ecdysone pulse.

IV. RT-qPCR

Quantitative reverse-transcription PCR (RT-qPCR) is a tool used to detect changes in gene expression, through measurement of a fluorescence (Adams,

2020). In order to prepare a sample for RT-qPCR, RNA is combined with Reverse Transcriptase, dNTPs, buffer, and Oligo(dT)s. Addition of these reagents results in the generation of cDNA. cDNA is then combined with DNA polymerase, gene-specific primers, buffer, dNTPs, and a fluorescent dye (SYBR Green) or probe (TaqMan detection). SYBR Green binds to double-stranded DNA during the extension phase, glowing more brightly the more DNA there is to bind to. TaqMan probes contain both a fluorescent component as well as a 'quencher'; when the probe is intact, there is no fluorescence, and when it's cleaved, fluorescence is detected. The probe works by binding to single-stranded cDNA upstream of the primers. During extension, the synthesizing strand will reach the probe and cleave it, activating the fluorescence.

Fluorescence is quantified as a Ct, or Cycle Threshold (this term is used interchangeably with Cq, or Cycle Quantification). For either the fluorescent dye or probe, the Ct is the point at which target gene fluorescence exceeds the threshold. The threshold, also called a baseline, is the fluorescence measured in the first 5-15 cycles of RT-qPCR, before any significant amplification has occurred. A lower Ct indicates a higher level of target gene amplification, since it would take fewer cycles to detect a higher concentration of material.

V. Hypothesis and Study Goals

Previous research performed in the Woodard Lab (Cavale, 2023) has found that *Dronc* expression was higher in larval cells undergoing PCD (the salivary glands) than in those not destroyed by PCD (the fat bodies). However,

this difference lacked statistical significance. It is my primary objective to expand this data set in efforts to further our understanding of the gene and caspase *Dronc*, and determine whether there is a correlation between expression of the gene *Dronc* and PCD.

My secondary objective concerns the spread of ecdysone through the pupa. *D. melanogaster* salivary glands are in the anterior end of the pupa, whereas the fat body is found throughout the pupa, in both anterior and posterior positions. During pupal development, the flow of ecdysone within the salivary glands begins from the ring gland at the anterior end. This has the effect of symmetric caspase activation in the salivary gland cells closest to the anterior end, with activation slowly spreading to the posterior cells (Takemoto et al., 2007).

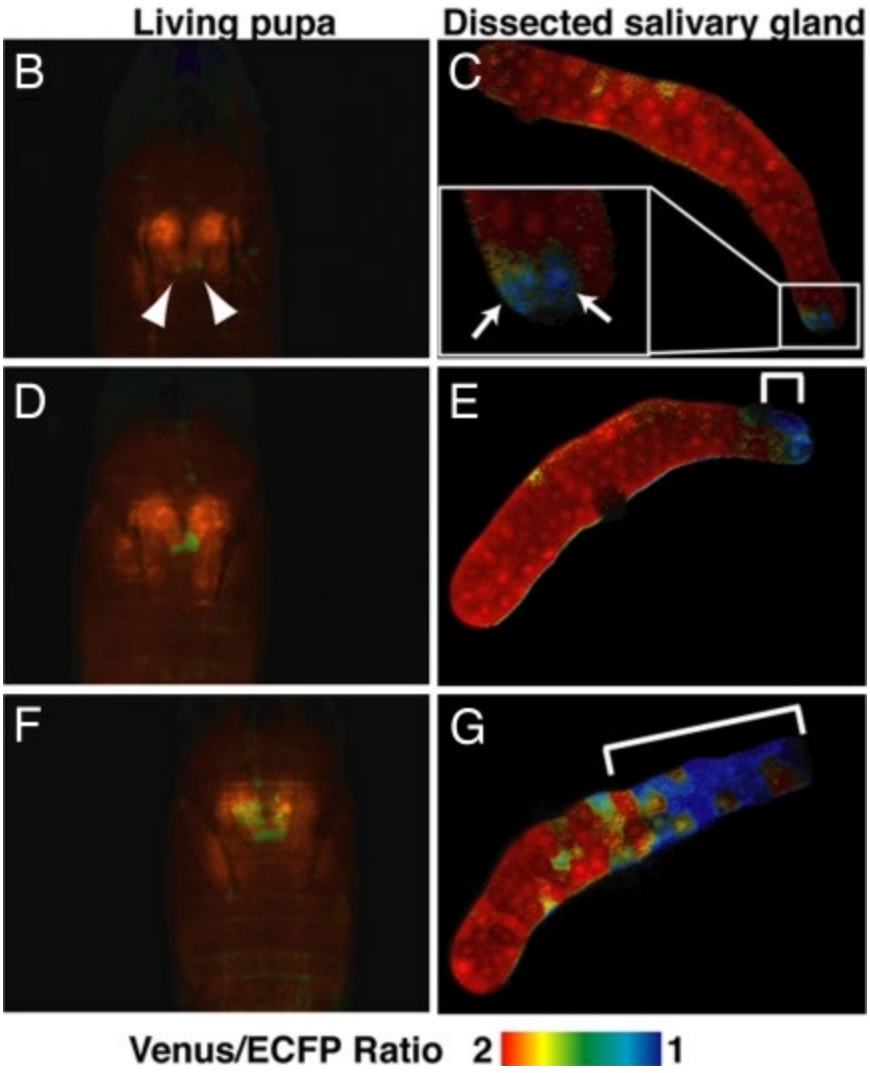

Figure 9. Confocal microscopy of activation of caspases in the salivary gland, in response to ecdysone exposure. Dissected salivary glands (C, E, G) display caspase activation initially in the anteriormost portion (closest to the ring gland), progressing to the posterior cells over time. This trend was also observed in living pupae (Takemoto et al., 2007).

Interestingly, when salivary glands are exposed to ecdysone *ex vivo*, this anterior-posterior spatiotemporal gradient is absent, with cell death occurring in random patterns. During dissection of pupal *Drosophila melanogaster* salivary

glands, one must isolate them from the specimen, and usually pull off a few fat body cells that have ‘stuck’ onto the salivary glands. Local exposure to ecdysone will interrupt the anterior to posterior tissue degradation of the salivary glands, but what is the effect of local exposure to ecdysone in the fat body? It has been shown that after 6 APF, fat body cells begin to dissociate from the anterior to the posterior direction (Nelliot et al., 2006). There is also evidence that even after anterior fat body cells have dissociated into the capsule (around 12 hrs. APF), there is little mixing of the fat bodies (Nelliot et al., 2006). Adipocytes which were in the anterior position in prepupae were later detected in the same anterior region of the pupae. If these fat body cells have been in contact with an area of high ecdysone concentration, would they still be a reliable control for a gene activated by ecdysone? My hypothesis is that fat body tissue harvested from the anterior end of the *D. melanogaster* pupa at 10-12 hrs. APF will have a higher expression of the gene *Dronc* due to their proximity to the source of ecdysone.

MATERIALS AND METHODS

I. Fly Maintenance

CS (Canton-S) flies of w^{1118} ("wild-type" control) genotype were used to provide larvae for dissection. They were raised at 25°C with 50% humidity on standard culture medium. Cavale used Genesee Scientific Nutri-Fly R Bloomington Formulation, and so that is what I used, for the sake of consistency between our experiments. The flies were transferred into new vials every 3-5 days to maintain freshness.

II. Dissection, Sample Collection, and Sample Label Classification

The flies chosen for dissection were first selected at the 0 APF stage, when the prepupa has just formed. This is identifiable by the expressed spiracles and initial pupal cuticle formation, while still retaining the white color of larvae. Around 8-10 prepupae were selected each session, and placed onto a damp piece of filter paper on a petri dish. This petri dish was then put in an incubation box and left in the incubator at 25°C. After 10 hours, half of the prepupae were dissected for their tissues and used as 10 hrs. APF samples, and 2 hours later the other prepupae were likewise used for 12 hrs. APF samples. This was done so that when comparing gene expression between 10 and 12 hrs. APF timepoints, there would be accuracy in comparing ages of prepupae relative to each other.

Dissections designated for 10 hrs. APF were dissected in the 30-minute window of 15 minutes before and after the 'exact' 10 hour point. The same process was respectively followed for the 12 hrs. APF samples. 2-3 individuals

were dissected for each sample, and when time permitted, a second sample at the same timepoint could be collected at the same timepoint. This is why some samples are labelled as having the same collection date, being differentiated by labels ‘A’ and ‘B’.

In order to differentiate between anterior and posterior fat body tissues, I have detailed the dissection techniques below, with photographs taken at every step. This is to ensure that in my collection of fat body tissues, there is a uniform classification of anterior and posterior. The classification is not exact; the purpose of comparing the two extremes (anterior and posterior) is to determine whether the spatiotemporal ecdysone gradient affects the fat body as a control tissue. Ideally, by comparing these two extremes, it would be possible to determine if further, more anatomically specific, dissection methods are required.

Dissection began with horizontal bisection of the pupa. The side with the spiracles is anterior, with the other side being posterior. In my collections of these tissues, I aimed to collect ‘anterior’ tissue from the anteriormost point of the anterior segment, primarily harvesting the fat body tissues off of salivary glands. The goal was to collect fat body tissues which were as close to the salivary glands as possible; when this was not, fat body tissues from the surrounding anterior portion were used. Ecdysone is released from the ring gland at the top of the salivary glands, and so fat body tissue on or around the salivary glands would be in closer proximity to the source of ecdysone.

For the posterior end, fat body tissues were collected from the posteriormost point. The bisection of the pupa was never exact, only intending to separate the two ends. This is because the fat body tissues were collected from the extreme of each point (anterior and posterior), with the initial bisection serving as a way to keep tissues from mixing unnecessarily. All dissection photos were taken with a 0 APF pupa for ease of identification and explanation, since at 10 and 12 hrs. APF the tissues have begun to degrade and separate.

The dissection process began with selection of pupae at zero hours post puparium formation (0 APF). These are identifiable as having already climbed the walls and formed the pupa, but still having a white appearance (Fernández-Moreno et al., 2007). Pupae further along in this process will have darkened in color. These 0 APF pupae were transferred to a petri dish with wet filter paper at the bottom, in order to maintain moisture. Half the pupae were incubated at 25 degrees Celsius for 10 hours, and the other half were aged for 12 hours in identical conditions.

Dissection began with pipetting 30 μL of PBS (Phosphate Buffer Solution) onto a dissection slide, and transferring the pupa onto the slide.

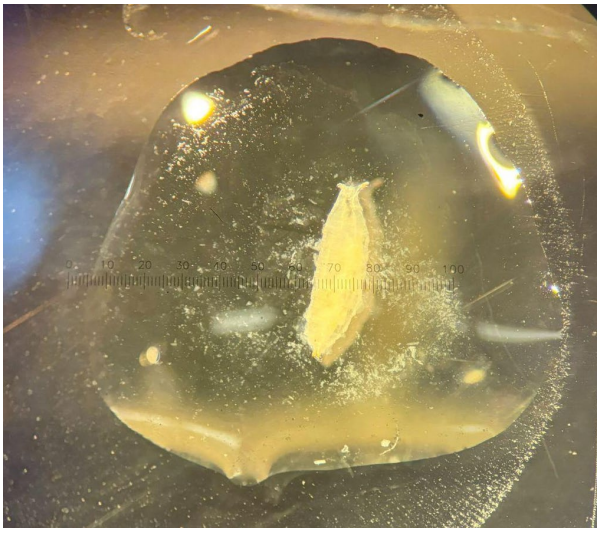

Figure 10. *Drosophila melanogaster* 0 APF prepupa suspended in 1X PBS under 10X optical with 1.5x magnification on an Olympus dissecting microscope. Photo taken with an iPhone 13 camera.

At this point, I took two pairs of tweezers to use as my dissection tools. I used one tweezer to hold the body steady, while the other tweezer gently pulled on the anterior larval spiracles in order to separate the salivary glands. When this step was done slowly and carefully, it was possible to simply pull the spiracles off and have the salivary glands attached to it, as shown below. The spiracles were carefully removed with tweezers.

I was then able to proceed with isolating the desired tissue and transferring it to a microcentrifuge tube with 30 µL PBS. Sometimes, during salivary gland dissection, pieces of the fat body will remain connected to the salivary gland. When possible, these were used as the anterior fat body sample, due to their proximity to the salivary glands. When this was not possible, anterior fat body tissues were collected as the fat body tissues that burst out of the pupa during

salivary gland removal. For the sample of salivary glands, the spiracles and all other non-salivary gland tissue were removed before transferring the tissue to a microcentrifuge tube.

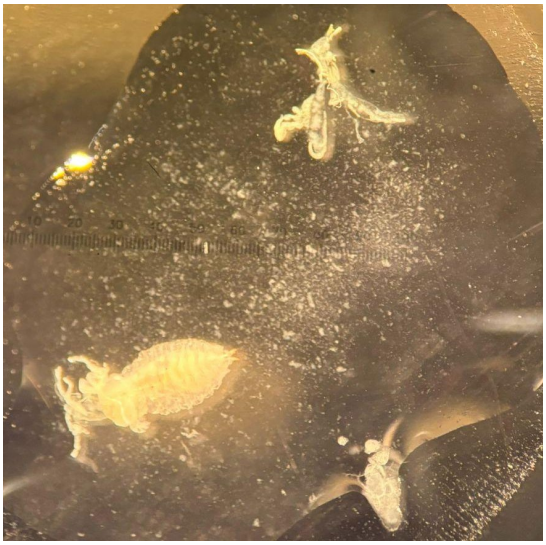

Figure 11. A 0 APF prepupa with spiracles attached to the salivary gland (top right) and the rest of the pupa (bottom left) in PBS under 10X optical with 1.5x magnification on an Olympus dissecting microscope. Photo taken with an iPhone 13 camera.

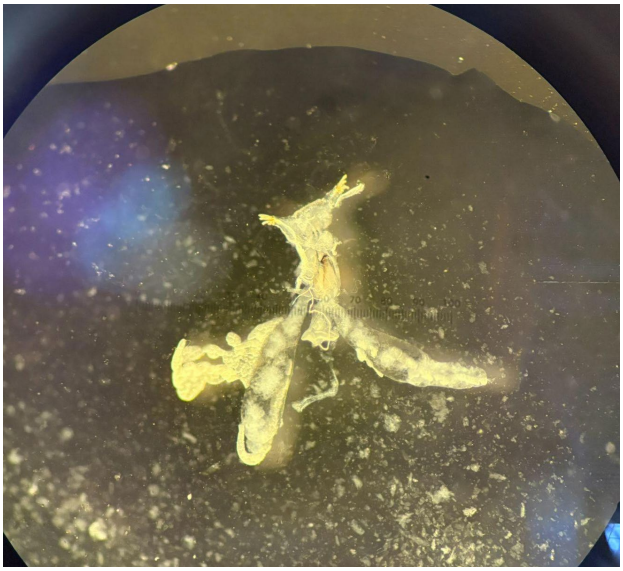

Figure 12. A 0 APF salivary gland with attached fat body and spiracles in PBS under 10X optical with 1.5x magnification on an Olympus dissecting microscope. Photo taken with an iPhone 13 camera.

Figure 13. A 0 APF salivary gland with attached fat body, post spiracle removal, in PBS under 10X optical with 1.5x magnification on an Olympus dissecting microscope. The fat body is highlighted in yellow, and the salivary gland is highlighted in blue. Photo taken with an iPhone 13 camera.

For collection of the posterior fat body, the pupa was cut roughly in half horizontally with tweezers, separating the anterior and posterior ends. The

posterior half was dragged to the opposite side of the dissection slide, and pushed gently to extrude the internal organs. Figure 5 shows how the bisections were performed.

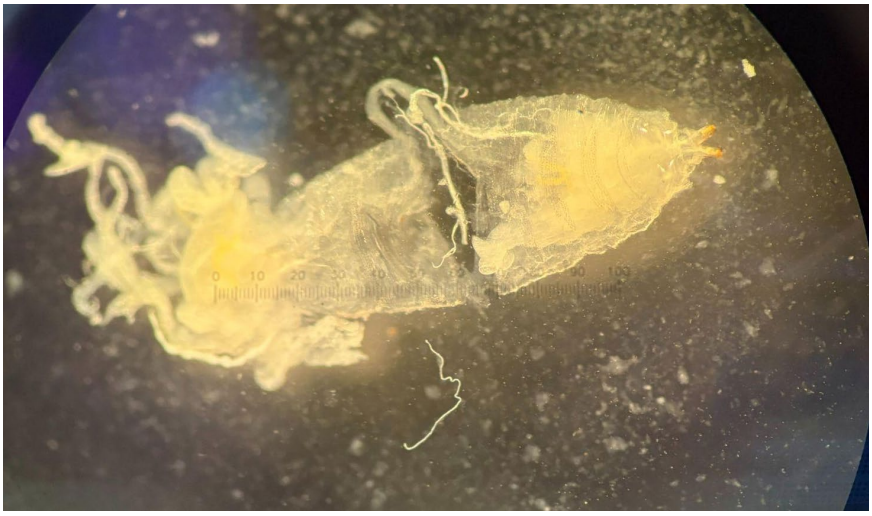

Figure 14. A 0 APF prepupa cut horizontally in half in PBS under 10X optical with 1.5x magnification on an Olympus dissecting microscope. The posterior end is to the right, seen with organs still inside. Photo taken with an iPhone 13 camera.

Between Figures 5 and 6, the posterior half of the fly pupa was dragged to a portion of the slide away from the anterior portion. This was done so that when collecting posterior fat body tissues, I could be certain that I was not taking samples of the anterior segment.

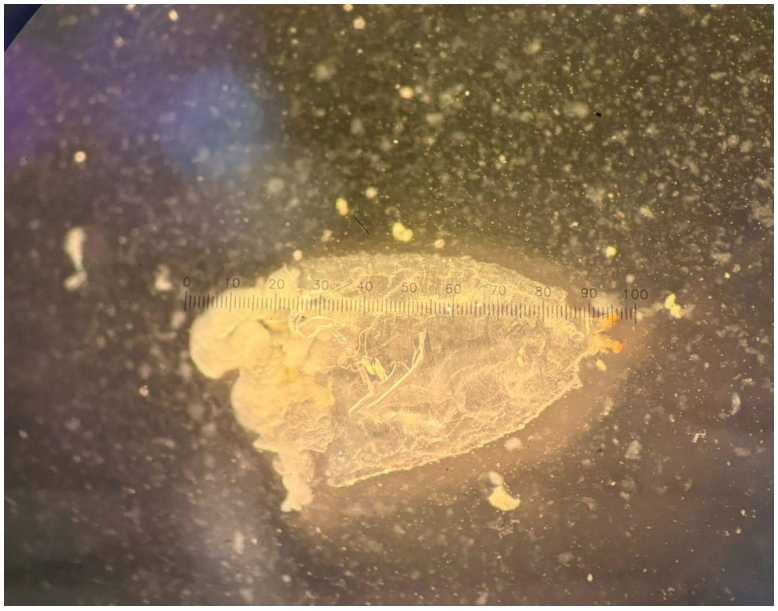

Figure 15. A 0 APF prepupa posterior in PBS under 10X optical with 1.5x magnification on an Olympus dissecting microscope. Photo taken with an iPhone 13 camera.

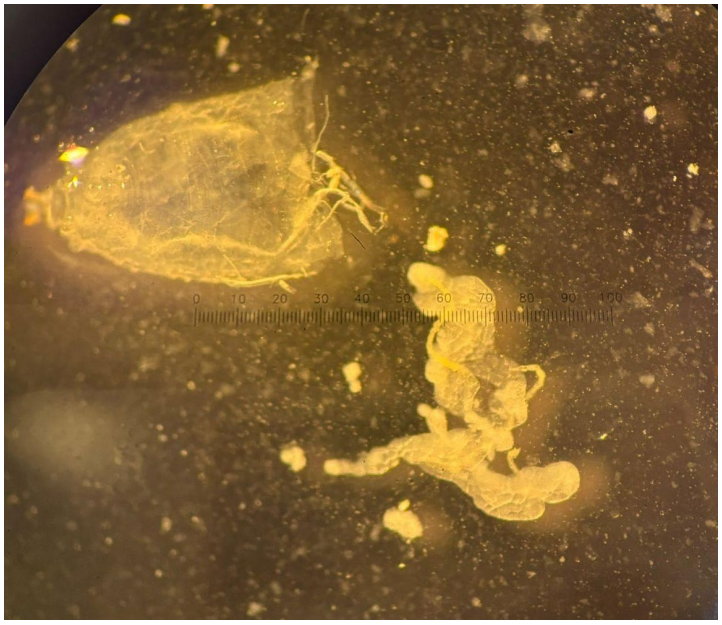

Figure 16. 0 APF prepupa posterior end with internal organs extruded. In PBS under 10X optical with 1.5x magnification on an Olympus dissecting microscope. Photo taken with an iPhone 13 camera. This photo demonstrates the method of fat body retrieval from the segment of the pupa designated ‘posterior’.

Once dissected, each tissue sample was transferred into a 1.5 µL microcentrifuge tube containing 30 µL PBS. Each sample contained tissues of 2-3 individual pupae.

III. RNA Isolation

300 µL TRIzol (Invitrogen) was added to each sample, and the sample was homogenized via a plastic homogenizer. For each sample, a 2 mL Phase Lock Gel-Heavy (Invitrogen) tube was placed in the centrifuge for 1 minute at 12,000 rpm. Each sample was then transferred into a tube with Phase Lock Gel, combined with 60 µL chloroform (Thermo-Fisher), and shaken thoroughly. Then, the samples were centrifuged at 2-8˚C for 10 minutes at 12,000 rpm. If clear phasing was visible in the top layer, the samples were moved to new microcentrifuge tubes, and mixed with 160 µL isopropanol (Sigma Aldrich). These were stored overnight at -20˚C.

The next day, the samples were thawed and placed in a centrifuge for 30 minutes at 13,400 rpm. After this step, small RNA pellets were visible at the bottom of the tubes. The supernatant was removed from these tubes via pipette to isolate the RNA pellets. Then, they were centrifuged again for 10 minutes at 13,400 rpm. The supernatant was again removed, and the pellets allowed to air-dry for 1 minute before being dissolved in 5 µL nuclease-free water.

IV. DNAse treatment

For each 10 µL sample of RNA, 1 µL of 10X DNase buffer (Ambion) and 1 µL rDNase-I (Ambion) were added. The samples were mixed by flicking and

were centrifuged for 1 minute. The samples were then incubated at 37˚C for 25-30 minutes. Then, 2 µL freshly vortexed DNase Inaction Reagent (Ambion) was added to each sample and allowed to sit at room temperature for 2 minutes, mixing intermittently. After, the samples were put in the centrifuge for 90 seconds at 10,000 rpm. Then, the supernatant of each sample was transferred to a clean vial, which could then be assessed for RNA concentrations.

It should be noted that treatment of RNA with DNase I can decrease the concentration of the sample (Norhazlin et al., 2015). However, treatment of RNA with DNase I still reduces amounts of residual DNA from the sample.

V. cDNA Synthesis

Synthesis of cDNA proceeded after isolation and DNase treatment of RNA samples. Since analysis is to take place via RT-PCR, the negative control in this case was a sample that lacks RT (Reverse Transcriptase). All of the samples were labeled. A first master mix was prepared, with the reagents listed below. Six reactions worth of master mix were prepared for the +RT condition, and six reactions worth of master mix for the -RT.

Table 1. Reagents for cDNA synthesis; master mix 1

Reagent	Amount per Reaction
RNA	1 µL
10 mM dNTP mix (Invitrogen)	1 µL
0.5 µg/µL oligo (dt) primer (Invitrogen)	1 µL
DEPC-treated water (Fisher Bioreagents)	7 µL

After the addition of RNA, the samples were labeled and incubated at 65˚C for 5 minutes, then placed on ice. Master Mix 2 was prepared for 12 reactions, with the reagents shown in Table 2.

Table 2. Reagents for cDNA synthesis; master mix 2

Component	Amount per Reaction
10X RT buffer (Invitrogen)	2 µL
25 mM MgCl 2 (Invitrogen)	4 µL
0.1 M DDT (Invitrogen)	2 µL
RNaseOUT (40 U/µL) (Invitrogen)	1 µL

9 µL of master mix 2 were added to each RNA/master mix 1 combination tube. The tubes were briefly centrifuged, before being placed in the incubator at 42˚C for 2 minutes. Then, 1 µL of SuperScript II RT was added to the six tubes labelled +RT, and 1 µL of DEPC-treated water was added to the six tubes labelled -RT. These tubes were mixed, centrifuged, and incubated at 42˚C for 50 minutes,

then terminated at 70˚C for 15 minutes. They were then incubated a final time at 37˚C for 20 minutes, before storage at -20˚C prior to further experiments.

VI. RT-PCR and Gel Electrophoresis

Polymerase chain reaction was used for amplification of specific sequences in the cDNA. PCR amplifies the DNA, and gel electrophoresis is able to later detect the gene specific products. A master mix was prepared before performing PCR, with the reagents in Table 3 below. After addition of 2 µL cDNA to the master mix per sample, they were then placed into the thermocycler (Table 4). The primers used were *Actin 5C* (Integrated DNA Technologies) and *Dronc* (Integrated DNA Technologies), and the master mix was prepared for 12 reactions.

Table 3. Reagents for RT-PCR

Component	Amount per Reaction
10X PCR Buffer -MgCl2 (Thermo Fisher)	5 µL
50 µM MgCl2 (Thermo Fisher)	3 µL
10 mM dNTPs (Thermo Fisher)	1 µL
10 µM reverse primer	2 µL
10 µM forward primer	2 µL
cDNA	2 µL
Nuclease-free water	34.6 µL
Taq Polymerase 0.4 µL (Thermo Fisher)	0.4 µL

Table 4. RT-PCR Thermocycler Profile

Stage	Temperature	Duration	Cycle Count
Denaturation	94°C	30 seconds	35 cycles
Annealing	56°C	30 seconds	35 cycles
Extension	72°C	30 seconds	35 cycles
Final Extension	72°C	5 minutes	1 cycle
Final Hold	4°C		

After processing in the thermocycler, the samples were ready for gel electrophoresis. The gel was made by combining and heating 0.8g agarose (Fisher Bioreagents), 50mL TAE, and 5 µL Gel Red DNA Stain (Biotium). This mixture was poured into a standard gel mold. The first well contained a 100 bp DNA ladder (Biotium) for reference. 18 µL of each RT-PCR material was combined with 2 µL loading dye (Biotium), and these were loaded into the gel. The electrophoresis ran for approximately 30 minutes, and the results were analyzed via LAS-3000 Luminescence Image Analyzer. After the results were deemed successful, the samples could be used for RT-qPCR.

VII. Real-Time Quantitative PCR

RT-qPCR is a quantitative process used for the amplification of and quantification of the gene of interest. As this reaction proceeds, RT-qPCR measures the amount of DNA amplified during each cycle. This is measured through a fluorescent dye, SYBR Green, which binds to dsDNA products and fluoresces brighter as more products are made. RT-qPCR results are measured by

Cycle Quantification, Cq, sometimes called Cycle Threshold, Ct. This is the number of PCR cycles that are required for the sample's fluorescence to noticeably rise above the threshold of background noise. Therefore, higher gene expression would result in a lower Cq.

Table 5. RT-qPCR Master Mix

Reagent	Amount Per Reaction
PowerUp SYBR Green (Thermo Fisher)	12.5 µL
10 µM forward primer	1.0 µL
10 µM reverse primer	1.0 µL
cDNA	1.0 µL
Nuclease-free water	9.5 µL

The primers used were *Dronc* for the experimental condition, and *Actin 5C* for the control. The target tissues were the anterior and posterior fat body, and the reference was the salivary gland. Samples were run in duplicate and the average of the Cq values was used to calculate the expression ratio. A 96-well plate was used, and the first two rows of the plate were used to determine the standard curves and efficiencies of the primers; the dilutions were 1/2, 1/4, 1/8, and 1/16. All RT-qPCR was performed using an AriaMx instrument.

Table 6. Layout of the 96-well plate for RT-qPCR. A1 to A5 are for the *Actin 5C* standard curve, and B1:B5 are for the *Dronc* standard curve. All other wells are labelled by primer. SG stands for Salivary Glands, AFB is Anterior Fat Body, and PFB is Posterior Fat Body. 10 and 12 hour APF samples are labeled 10 and 12. Column 4 from C through H is left intentionally blank.

	1	2	3	4	5	6	7
A	1/1 *Actin*	1/2 *Actin*	1/4 *Actin*	1/8 *Actin*	1/16 *Actin*		
B	1/1 *Dronc*	1/2 *Dronc*	1/4 *Dronc*	1/8 *Dronc*	1/16 *Dronc*		
C	*Actin* +RT 10 SG	*Actin* +RT 10 SG	*Actin* -RT 10 SG		*Actin* +RT 12 SG	*Actin* +RT 12 SG	*Actin* -RT 12 SG
D	*Actin* +RT 10 AFB	*Actin* +RT 10 AFB	*Actin* -RT 10 AFB		*Actin* +RT 12 AFB	*Actin* +RT 12 AFB	*Actin* -RT 12 AFB
E	*Actin* +RT 10 PFB	*Actin* +RT 10 PFB	*Actin* -RT 10 PFB		*Actin* +RT 12 PFB	*Actin* +RT 12 PFB	*Actin* -RT 12 PFB
F	*Dronc* +RT 10 SG	*Dronc* +RT 10 SG	*Dronc* -RT 10 SG		*Dronc* +RT 12 SG	*Dronc* +RT 12 SG	*Dronc* -RT 12 SG
G	*Dronc* +RT 10 AFB	*Dronc* +RT 10 AFB	*Dronc* -RT 10 AFB		*Dronc* +RT 12 AFB	*Dronc* +RT 12 AFB	*Dronc* -RT 12 AFB
H	*Dronc* +RT 10 PFB	*Dronc* +RT 10 PFB	*Dronc* -RT 10 PFB		*Dronc* +RT 12 PFB	*Dronc* +RT 12 PFB	*Dronc* -RT 12 PFB

It should be noted that each condition is run in duplicate, as opposed to the standard triplicate. This was done due to the large volume of reagents needed for

the multiple variables being measured (*Dronc* vs *Actin* primers, salivary glands, anterior and posterior fat body, positive and negative control, 10 vs 12 hrs. APF). Additionally, the reagents for RT-qPCR are expensive, and this experiment was performed in a lab space where RT-qPCR reagents were shared between multiple researchers. Therefore, the experiment was run in duplicate. While this may make interpretation of results difficult, the coefficient of variation (CV) for each datapoint's two Cq values can provide clarity as to reliability of the measured expression. CV values will be shown alongside the averaged and individual Cq values for each datapoint, in Appendix 1.

VIII. Real-Time Quantitative PCR Data Analysis

Pfaffl (2001) developed a method for analyzing qPCR results and primer efficacy. This method was used to quantify the expression of *Actin 5C* and *Dronc*. This is done in order to assess gene expression in relation to each primer's individual efficiencies. The Pfaffl equation below was used to determine the relative expression ratio of a target gene in comparison to a reference gene:

$$\text{ratio} = \frac{(E_{\text{target}})^{\Delta \text{CP}_{\text{target}}(control - sample)}}{(E_{\text{ref}})^{\Delta \text{CP}_{\text{ref}}(control - sample)}}$$

E_{target} was *Dronc* efficiency, and E_{ref} was *Actin 5C* efficiency. ΔCP_{target} was the fat body cells (either posterior or anterior) and $\Delta CP_{reference}$ was the salivary gland cells. Due to complications and errors with procedure, most of the data collected does not have a standard curve, and so an ideal primer efficiency of 2

was assumed in the calculations. For those calculations the double delta Cq method was used to quantify the gene expression. This method raises -ΔΔCq to the power of the assumed expression, which is 2. ΔΔCq the difference between two delta values. Take the Cq of the gene of interest in experimental conditions, and subtract it by the Cq of the housekeeping gene in the experimental conditions- this is the first ΔCq, the ΔCq of experimental conditions. Then, take the Cq of the gene of interest in control conditions and subtract it by the Cq of the housekeeping gene in control conditions- this is the ΔCq of control conditions. To get ΔΔCq, subtract the Cq of control conditions from the Cq of experimental conditions.

Each datapoint is the ratio of *Dronc* expression in the anterior or posterior fat body over the *Dronc* expression in the salivary glands. Therefore, a value of 1 would mean that there is equal *Dronc* expression in the experimental and control tissues, a value of less than 1 means the experimental tissue has less *Dronc* expression than the control, and a value greater than 1 means the experimental tissue has higher *Dronc* expression than the control.

RESULTS

I. RNA Isolation

RNA was evaluated for purity via nanodrop spectrophotometer. The OD260/280 ratios and OD260/230 were sufficiently high to proceed with cDNA synthesis.

Report Configuration Print

Sample ID	User name	Date and Time	Nucleic Acid	Unit	A260 (Abs)	A280 (Abs)	260/280
3-3-sb10	Phoebe Grabowski	4/17/2025 11:53 AM	113.6	ng/µl	2.841	1.615	1.76
3-3-b10	Phoebe Grabowski	4/17/2025 11:54 AM	93.8	ng/µl	2.344	1.278	1.83
3-3-b12-b	Phoebe Grabowski	4/17/2025 11:59 AM	141.9	ng/µl	3.547	2.298	1.54
3-3-s12	Phoebe Grabowski	4/17/2025 11:55 AM	146.0	ng/µl	3.650	2.309	1.58
3-3-sb12	Phoebe Grabowski	4/17/2025 11:56 AM	129.6	ng/µl	3.241	1.919	1.69
3-3-b12	Phoebe Grabowski	4/17/2025 11:56 AM	158.8	ng/µl	3.971	2.350	1.69
3-3-s10-b	Phoebe Grabowski	4/17/2025 11:57 AM	174.0	ng/µl	4.351	2.729	1.59
3-3-sb10-b	Phoebe Grabowski	4/17/2025 11:57 AM	134.9	ng/µl	3.372	1.974	1.71
3-3-b10-b	Phoebe Grabowski	4/17/2025 11:58 AM	219.8	ng/µl	5.495	2.933	1.87
3-3-s12-b	Phoebe Grabowski	4/17/2025 11:58 AM	103.7	ng/µl	2.592	1.604	1.62
3-3-sb12-b	Phoebe Grabowski	4/17/2025 11:59 AM	121.9	ng/µl	3.049	1.769	1.72

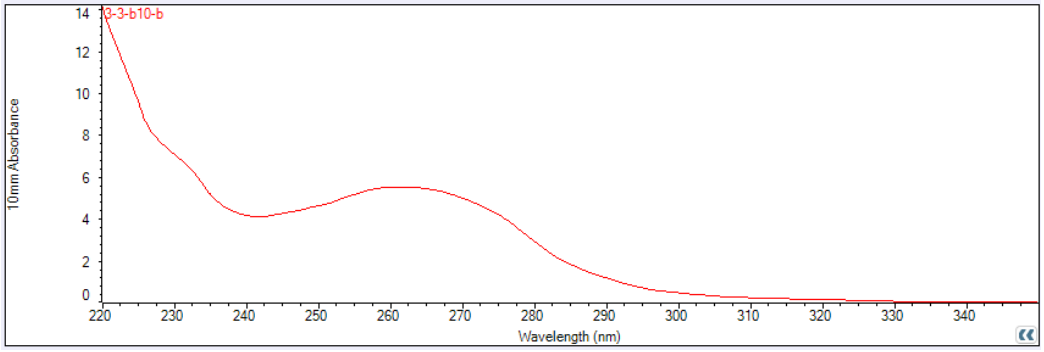

Figure 17. Screenshot of nanodrop spectrophotometer graph showing absorbance values of the RNA samples.

The OD260/280 ratios were deemed acceptable at 1.5 and above, though samples with values below 1.5 were still used due to difficulty achieving consistent RNA purity. The typical minimum OD260/280 value is 1.7, but due to a lack of high-quality RNA samples, this benchmark was arbitrarily decreased to 1.5. The results for data excluding the samples with subpar OD260/280 RNA ratios will be shown

separately. Information on exact RNA OD260/280 ratios can be found in Appendix 2.

II. PCR Products and Gel Electrophoresis

An agarose gel was loaded with PCR-amplified samples of *Actin 5C* and *Dronc* primers to test primer viability (Figure 8). Each sample is identified in the drawing alongside this figure.

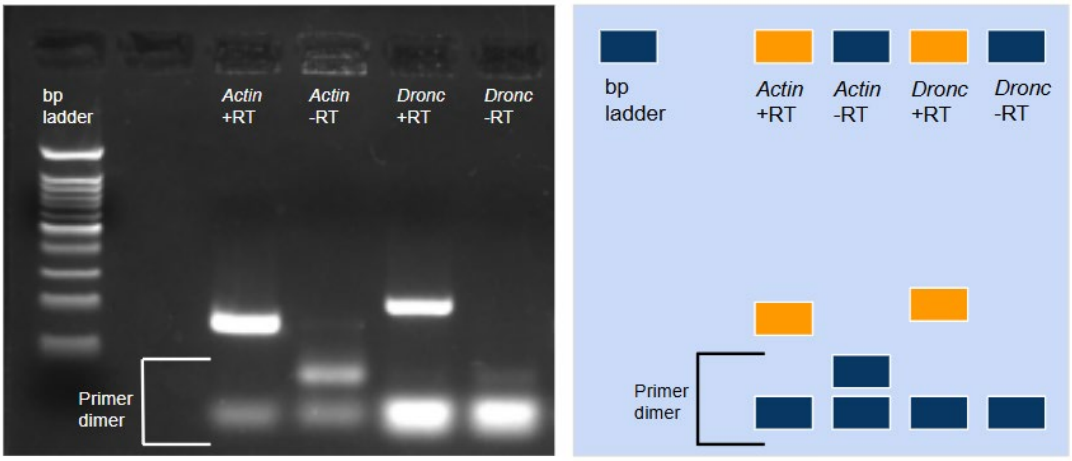

Figure 18. Gel electrophoresis results. (Left) Photograph of gel electrophoresis, labeled by gene used. Residual bands below 100 bp are primer-dimers. (Right) The highlighted wells on the right, in orange, represent the +RT samples. The lines in the gel show that these primers, both *Actin 5C* (158 bp) and *Dronc* (214 bp), were effective.

III. Quantitative Real-Time PCR Standard Curves

Each RT-qPCR plate contained the reactions for standard curves for each pair of primers, though this was only effective for two of the RT-qPCR runs. The standard curve reactions included as templates, a serial dilution of WT cDNA: 1/1, 1/2, 1/4, 1/8, 1/16, and was performed for both *Actin 5C* and *Dronc*. The Pfaffl equation was used to account for errors in primer efficiency, and how that

would affect the expression ratios. Data from the standard curve was plotted for each gene. An efficiency of 2 is considered ideal.

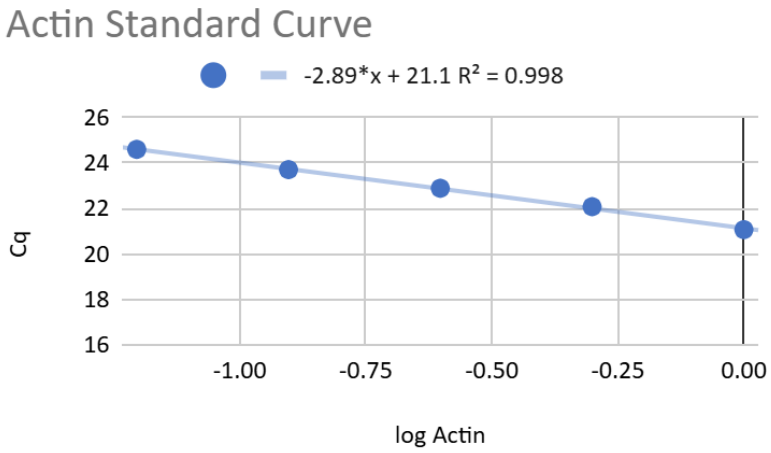

Figure 19. Standard Curve for *Actin 5C* primers. Depicts the standard curve results for the gene expression of *Actin 5C*, plotted on a log scale. The standard curve here was made with a sample of salivary glands from 10/27/24-B2. The slope is -2.89, which can be used to find efficiency of the primers with the equation Efficiency= 10^(-1/-[slope]). In this example, the *Actin 5C* primer efficiency is 2.218.

IV. RT-qPCR Expression Ratios

Due to the difficulty in producing a standard curve for the Pfaffl equation, there will be three sets of data presented. The first set is ideal, with only samples which were analyzed by the Pfaffl equation and which produced sufficient efficiency for both primers. The second set includes the aforementioned samples, as well as those for which an ideal primer efficiency of 2 was assumed. Through this, it will be possible to analyze the broader depth of data, while still highlighting the importance of correctly accounting for primer efficiency. Both of

these datasets include only samples for which the RNA OD260/280 ratio was 1.5 or higher.

The third dataset consists of all data collected, including those that may have been excluded due to an RNA OD260/280 ratio of less than 1.5, and those for which Tm (melting temperature) was unable to be measured. There are 2 RT-qPCR runs for which Tm was not measured by the computer, but for each sample where Tm was measured, there were no values less than 80. This data will be far less accurate, but provides an interesting insight for those who may recreate the experiment.

In the 'RNA>1.5' dataset, there are samples both with and without a standard curve. For samples in which the primer efficiency could be determined, the resulting expression ratio was used. The expression ratio is not assumed to be 2, alongside the datapoints for which an expression of 2 was a necessary assumption. The reasoning behind this is that when the best possible data is available, it should be used. Therefore, although it may be less internally consistent for 'RNA>1.5' as a dataset, use of the most accurate data (when possible) was prioritized.

Dronc **Fat Body/Salivary Gland Expression Ratios**

These are the results of individual RT-qPCR runs, with the ratios of anterior or posterior fat body expression over salivary gland expression at each timepoint. Due to high variance between anterior and posterior *Dronc* expression for both 10 and 12 hrs. APF, a two-way ANOVA was performed to determine

significance. It was only possible to perform the ANOVA on the 'RNA>1.5' and 'All Data' datasets, due to the low sample size of the most reliable samples.

Table 7. Best Data RT-qPCR ratios of fat body *Dronc* expression. This table shows the RT-qPCR expression ratios for each sample, using *Dronc* and *Actin 5C* primers. This data consists only of samples for which the RNA OD260/280 ratio was greater than 1.5, and for which a standard curve was achieved. A value of 1 means that *Dronc* and *Actin 5C* are equally expressed, a value less than 1 indicates underexpression of *Dronc* in the fat body, and a value greater than 1 indicates overexpression.

	10 hrs. APF Anterior FB/SG ratio	10 hrs. APF Posterior FB/SG ratio	12 hrs. APF Anterior FB/SG ratio	12 hrs. APF Posterior FB/SG ratio	Dronc Primer Efficiency	Actin Primer Efficiency
10/27/24-B2				1.597	2.904	2.218
2/14/25-A	0.746	2.305	1.189	1.46	2.04	1.972
Average	n/a	n/a	n/a	1.5285	2.472	2.095
Standard Deviation	n/a	n/a	n/a	0.09687362902	0.6109402589	0.1739482682
Standard Error	n/a	n/a	n/a	0.0685	0.432	0.123

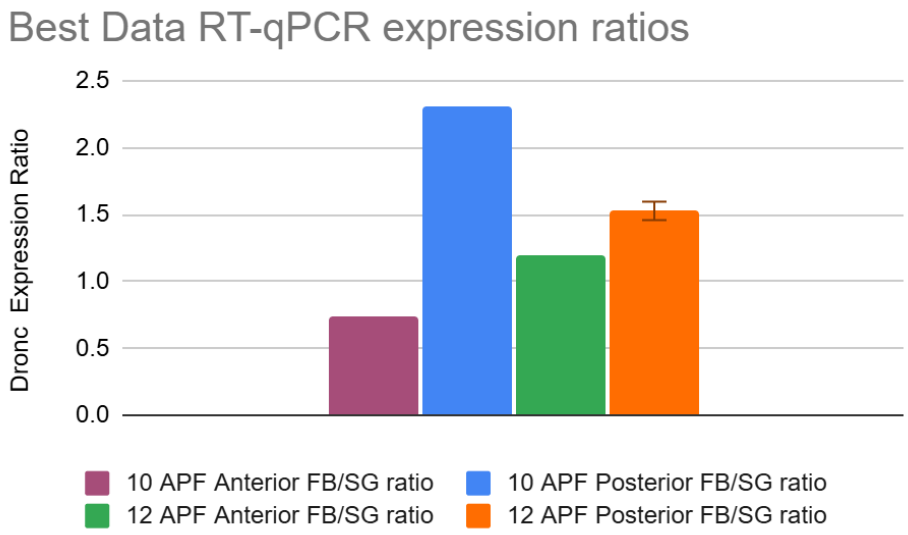

Figure 20. Best Data bar graph of RT-qPCR ratios of fat body *Dronc* expression. This graph shows the RT-qPCR expression ratios for each sample, using *Dronc* and *Actin 5C* primers. This data consists only of samples for which the RNA OD260/280 ratio was greater than 1.5, and for which a standard curve was achieved. When replicates of the same category are available, the standard error is expressed as an error bar.

This data represents the relative expression of *Dronc* in the fat body, as compared to the salivary gland. Using the most accurate data available, RT-qPCR detected underexpression of *Dronc* in the anterior fat body compared to salivary gland at 10 hours APF (meaning a higher expression in the salivary glands), and overexpression in the posterior fat body at 10 hrs. APF, as well as both anterior and posterior fat body at 12 hrs. APF. The most extreme difference in expression is in posterior fat body tissue at 10 hrs. APF, with a ratio of 2.305. The anterior *Dronc* expression in the fat body seems to be lower than in the posterior fat body tissues, at both 10 and 12 hrs. APF timepoints.

Table 8. Only data with RNA OD260/280 ratio >1.5 RT-qPCR ratios of *Dronc* expression. This table shows the RT-qPCR expression ratios for each sample, using *Dronc* and *Actin 5C* primers. This data consists only of samples for which the RNA OD260/280 ratio was greater than 1.5. When standard curve data was unavailable, an ideal primer efficiency of 2 was assumed. A value of 1 means that *Dronc* and *Actin 5C* are equally expressed, a value less than 1 indicates underexpression of *Dronc* in the fat body, and a value greater than 1 indicates overexpression.

	10 hrs. APF Anterior FB/SG ratio	10 hrs. APF Posterior FB/SG ratio	12 hrs. APF Anterior FB/SG ratio	12 hrs. APF Posterior FB/SG ratio	Dronc Primer Efficiency	Actin Primer Efficiency
10/27/24-A2	1.469	1.091			2 (assumed)	2 (assumed)
3/3/25-A	1.693	4.098	0.067	0.265	2 (assumed)	2 (assumed)
10/27/24-B2				1.597	2.904	2.218
2/14/25-A	0.746	2.305	1.189	1.46	2.04	1.972
Average	1.303	2.498	0.628	1.107	n/a	n/a
Standard Deviation	0.495	1.513	0.793	0.733	n/a	n/a
Standard Error	0.286	0.873	0.561	0.423	n/a	n/a

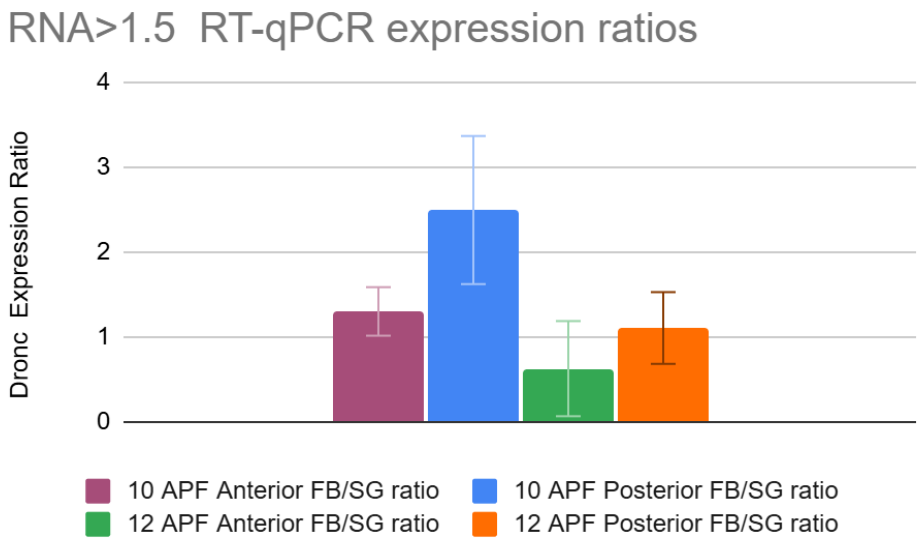

Figure 21. Only data with RNA OD260/280 ratio >1.5 bar graph of RT-qPCR ratios of *Dronc* expression. This graph shows the RT-qPCR expression ratios for each sample, using *Dronc* and *Actin 5C* primers. This data consists only of samples for which the RNA OD260/280 ratio was greater than 1.5. When standard curve data was unavailable, an ideal primer efficiency of 2 was assumed. The standard error is expressed through error bars.

Using all data points for which the RNA OD260/280 ratio was greater than 1.5, there was slight overexpression of *Dronc* in the 10 hrs. APF anterior fat body, and the 12 hrs. APF posterior fat body. There was underexpression of *Dronc* in the anterior fat body at 12 hrs. APF, with a ratio of 0.628. Here, once again, the most extreme difference in expression is the posterior fat body tissue at 10 hrs. APF, with a ratio of 2.498. For each respective timepoint, there seems to be a higher expression of *Dronc* in the posterior fat body, as opposed to an anterior portion of the fat body.

Table 9. Only data with RNA OD260/280 ratio >1.5 ANOVA Results. This table shows the results of the two-way ANOVA analysis of the *Dronc* expression ratios. This data consists only of samples for which the RNA OD260/280 ratio was greater than 1.5. When standard curve data was unavailable, an ideal primer efficiency of 2 was assumed. APF indicates if the expression ratio changes between 10 and 12 hrs. APF, Fat Body Position indicates whether the expression of *Dronc* in fat body tissue changes depending on anterior or posterior tissue collection, and APF:Fat Body Position indicates whether the effect on APF depends on the position of the fat body cells being anterior or posterior. Pr(>F) indicates the p-values.

	Df	Sum Sq	Mean Sq	F value	Pr(>F)
APF	1	2.645	2.6446	2.735	0.142
Fat Body Position	1	2.077	2.0772	2.148	0.186
APF:Fat Body Position	1	0.342	0.3418	0.353	0.571
Residuals	7	6.77	0.9671		

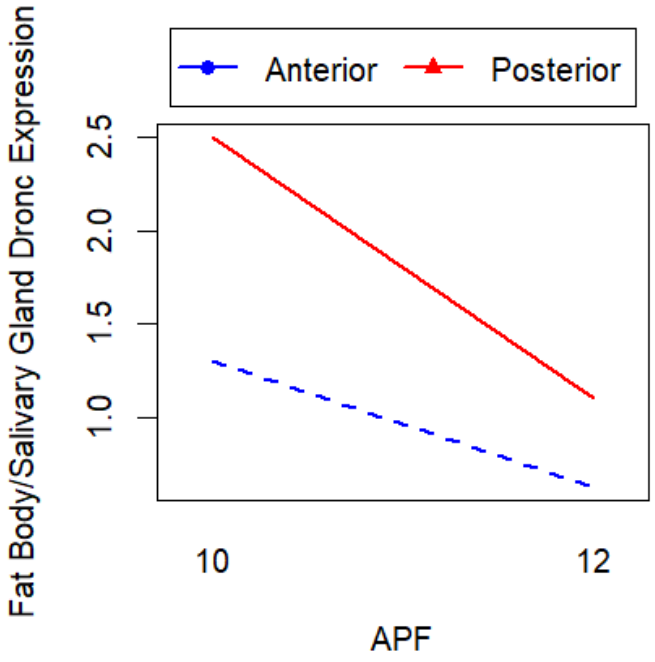

Figure 22. Only data with RNA OD260/280 ratio >1.5 ANOVA Graphical Representation. This graph shows the results of the two-way ANOVA analysis of the *Dronc* expression ratios. This data consists only of samples for which the RNA OD260/280 ratio was greater than 1.5. When standard curve data was unavailable, an ideal primer efficiency of 2 was assumed. *Dronc* expression in the fat body is the y-axis, while APF is the x-axis. The blue line indicates the trend for anterior fat body tissues, and the red line indicates the trend for posterior fat body tissues.

A two-way ANOVA was performed to determine significance of the effects of APF and fat body position (anterior or posterior) on the *Dronc* expression ratio. No significant effect of APF was observed ($p=0.142$), nor was there an observed significant effect of fat body position ($p=0.186$) on the expression ratios. There was also no significant interaction between APF and fat

body position (p=0.571). This ANOVA was performed only using the 'RNA>1.5' samples, and thus the low sample size of n=11 should be noted.

Table 10. All Data (regardless of OD260/280 value or lack of Tm measurement) RT-qPCR ratios of *Dronc* expression. This table shows the RT-qPCR expression ratios for each sample, using *Dronc* and *Actin 5C* primers. Data is presented here regardless of RNA OD260/280 value, or success in attaining a standard curve. Samples for which the Tm was not measured are marked with an asterisk, like so*. When standard curve data was unavailable, an ideal primer efficiency of 2 was assumed. A value of 1 means that *Dronc* and *Actin 5C* are equally expressed, a value less than 1 indicates underexpression of *Dronc* in the fat body, and a value greater than 1 indicates overexpression.

	10 hrs. APF Anterior FB/SG ratio	10 hrs. APF Posterior FB/SG ratio	12 hrs. APF Anterior FB/SG ratio	12 hrs. APF Posterior FB/SG ratio	Dronc Primer Efficiency	Actin Primer Efficiency
10/27/2024-A1*	0.059	0.175	0.449	0.774	2 (assumed)	2 (assumed)
10/27/24- A2	1.469	1.091	0.367	0.616	2 (assumed)	2 (assumed)
10/27/24-B1*	0.023	2.888	0.441	0.75	2 (assumed)	2 (assumed)
3/3/25- A	1.693	4.098	0.067	0.265	2 (assumed)	2 (assumed)
10/27/24- B2			3	1.597	2.904	2.218
2/14/25- A	0.746	2.305	1.189	1.46	2.04	1.972
Average	0.798	2.1114	0.9188333333	0.9103333333	n/a	n/a
Standard Deviation	0.7747122046	1.531178402	1.084753689	0.5140088196	n/a	n/a
Standard Error	0.3568764492	0.9442467855	0.3751121376	0.3716420271	n/a	n/a

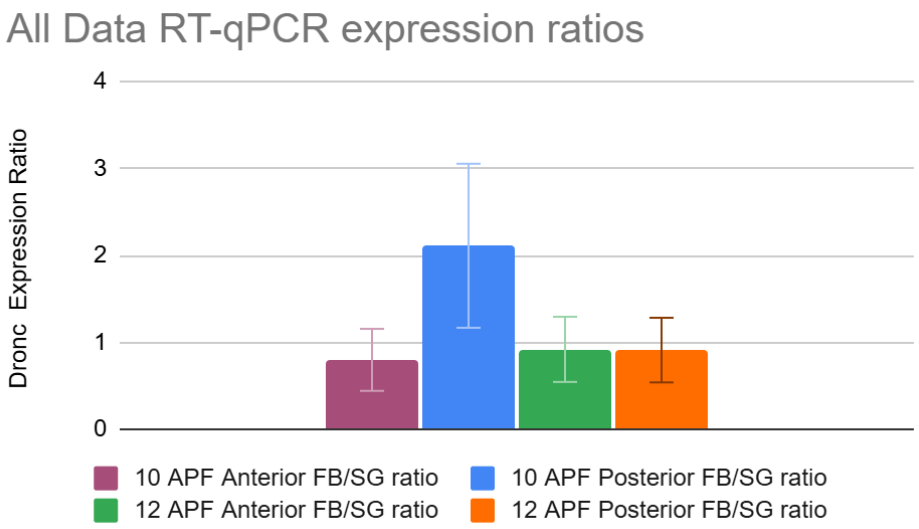

Figure 23. All Data (regardless of OD260/280 value or lack of Tm measurement) bar graph of RT-qPCR ratios of *Dronc* expression. This table shows the RT-qPCR expression ratios for each sample, using *Dronc* and *Actin 5C* primers. Data is presented here regardless of RNA OD260/280 value, success in

attaining a standard curve, or measurement of Tm. When standard curve data was unavailable, an ideal primer efficiency of 2 was assumed. The standard error is expressed through error bars.

The results from Figure 23 were obtained through analysis of unreliable samples. This would include those with RNA OD260/280 values of less than 1.5, those for which the Tm was not measured, and those for which a standard curve was not achieved. As such, these results should be regarded as questionable. There is once again a high level of *Dronc* overexpression in the posterior fat body at 10 hrs. APF. The anterior 10 hrs. APF as well as both 12 hrs. APF variables showed slight underexpression of *Dronc*.

Table 11. All Data (regardless of OD260/280 value or lack of Tm measurement) ANOVA Results. This table shows the results of the two-way ANOVA analysis of the expression ratios. Data is presented here regardless of RNA OD260/280 value, success in attaining a standard curve, or measurement of Tm. When standard curve data was unavailable, an ideal primer efficiency of 2 was assumed. APF indicates if the expression ratio changes between 10 and 12 hrs. APF, Fat Body Position indicates whether the expression of *Dronc* in fat body tissue changes depending on anterior or posterior tissue collection, and APF:Fat Body Position indicates whether the effect on APF depends on the position of the fat body cells being anterior or posterior. Pr(>F) indicates the p-values.

	Df	Sum Sq	Mean Sq	F Value	Pr(>F)
APF	1	1.591	1.591	1.509	0.235
Fat Body Position	1	1.93	1.93	1.83	0.193
APF:Fat Body Position	1	2.383	2.383	2.259	0.15
Residuals	18	18.983	1.055		

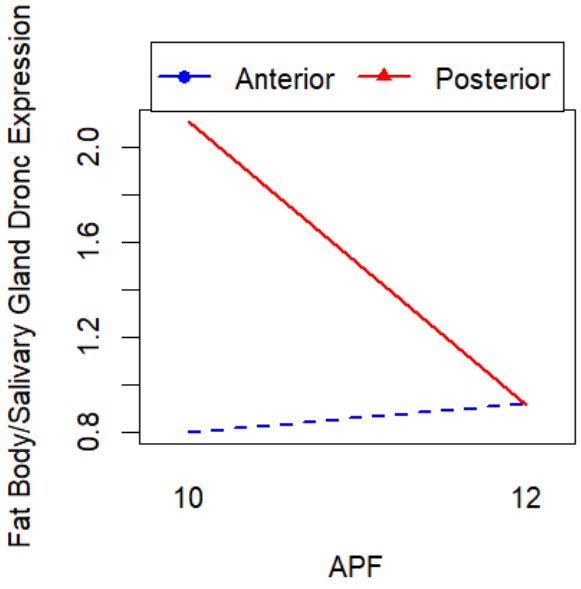

Figure 24. All Data (regardless of OD260/280 value or lack of Tm measurement) ANOVA Results. This graph shows the results of the two-way ANOVA analysis of the expression ratios. Data is presented here regardless of RNA OD260/280 value, success in attaining a standard curve, or measurement of Tm. When standard curve data was unavailable, an ideal primer efficiency of 2 was assumed. *Dronc* expression in the fat body is the y-axis, while APF is the x-axis. The blue line indicates the trend for anterior fat body tissues, and the red line indicates the trend for posterior fat body tissues.

A two-way ANOVA was performed to determine significance of the effects of APF and fat body position (anterior or posterior) on the *Dronc* expression ratio. No significant effect of APF was observed ($p=0.235$), nor was there an observed significant effect of fat body position ($p=0.193$) on the expression ratios. There was also no significant interaction between APF and fat body position ($p=0.15$).

Ratios of Anterior/Posterior Fat Body *Dronc* Expression

For comparison of anterior and posterior fat bodies, I chose to divide the anterior *Dronc* expression ratio by the posterior *Dronc* expression ratio. This method was chosen because it is a continuation of the double delta Cq method (Pfaffl, 2001). It also has the effect of normalizing the data, since expression varies drastically between samples. By attaining a ratio of anterior/posterior expression, it becomes possible to compare the results from multiple runs, without the concern of a high standard deviation. This normalized data is analyzed by a one-sided t-test, though this was only possible with the 'All Data' dataset due to

low sample number. If the expression is the same in both anterior and posterior fat body tissues, then the ratio should be equal to 1.

Table 12. Best Data *Dronc* Expression in the anterior fat body divided by that of the posterior fat body. This table shows the RT-qPCR expression ratios for each sample, using *Dronc* and *Actin 5C* primers. This is a direct comparison of anterior and posterior fat body *Dronc* expression. For both 10 and 12 hrs. APF, the results were attained by dividing the anterior fat body expression by the posterior fat body expression. This data consists only of samples for which the RNA OD260/280 ratio was greater than 1.5, and for which a standard curve was achieved. A value of 1 means that the anterior and posterior express *Dronc* equally, a value less than 1 indicates underexpression of *Dronc* in the anterior fat body, and a value greater than 1 indicates overexpression in the anterior fat body.

	10 hrs. APF anterior/posterior	12 hrs. APF anterior/posterior
2/14/35-A	0.3236442516	0.8143835616

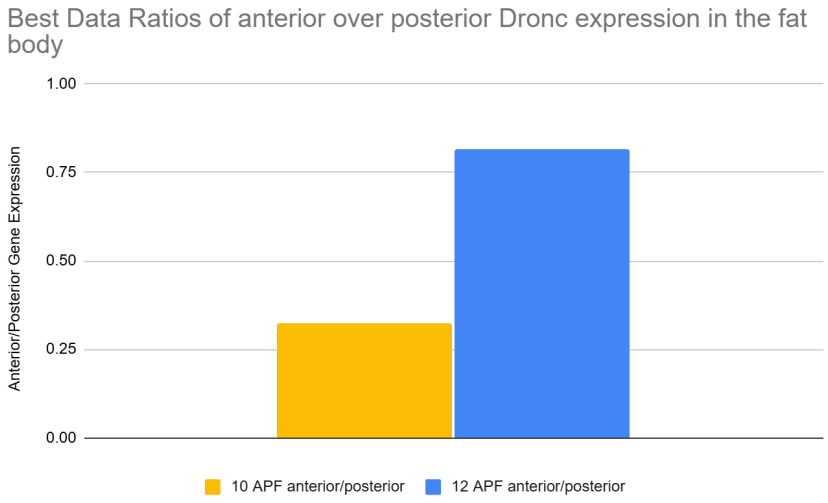

Figure 25. Best Data *Dronc* Expression in the anterior fat body divided by that of the posterior fat body, represented as a bar graph. This graph shows the RT-qPCR expression ratios for each sample, using *Dronc* and *Actin 5C*

primers. This is a direct comparison of anterior and posterior fat body *Dronc* expression. For both 10 and 12 hrs. APF, the results were attained by dividing the anterior fat body expression by the posterior fat body expression. This data consists only of samples for which the RNA OD260/280 ratio was greater than 1.5, and for which a standard curve was achieved.

Using the most reliable data, there is only a single RT-qPCR run from which answers can be interpreted. At 10 hrs. APF, there was an anterior/posterior *Dronc* expression ratio of 0.324, indicating overexpression in the posterior fat body cells. Similar results were found for 12 hrs. APF, though to a lesser degree, with a ratio of 0.814. This would indicate that there is a lesser difference between the anterior and posterior fat body *Dronc* expression at 12 hrs. APF, as compared to 10 hrs. APF.

Table 13. Only data with RNA OD260/280 ratio >1.5 *Dronc* Expression in the anterior fat body divided by that of the posterior fat body. This table shows the RT-qPCR expression ratios for each sample, using *Dronc* and *Actin 5C* primers. This is a direct comparison of anterior and posterior fat body *Dronc* expression. For both 10 and 12 hrs. APF, the results were attained by dividing the anterior fat body expression by the posterior fat body expression. This data consists only of samples for which the RNA OD260/280 ratio was greater than 1.5. When standard curve data was unavailable, an ideal primer efficiency of 2 was assumed. A value of 1 means that the anterior and posterior express *Dronc* equally, a value less than 1 indicates underexpression of *Dronc* in the anterior fat body, and a value greater than 1 indicates overexpression in the anterior fat body.

	10 hrs. APF anterior/posterior	12 hrs. APF anterior/posterior
10/27/24-A2	1.346471127	
3/3/25-A	0.4131283553	0.2528301887
2/14/35-A	0.3236442516	0.8143835616
Average	0.6944145781	0.5336068752
Standard Deviation	0.5664672619	0.397078198
Standard Error	0.283233631	0.2292532045

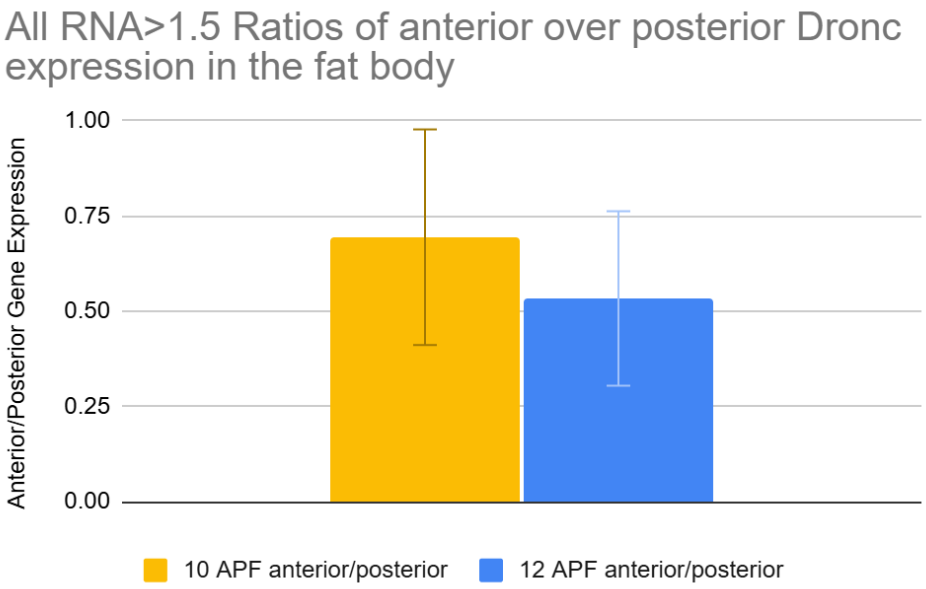

Figure 26. Only data with RNA OD260/280 ratio >1.5 *Dronc* Expression in the anterior fat body divided by that of the posterior fat body, represented as a bar graph. This graph shows the RT-qPCR expression ratios for each sample, using *Dronc* and *Actin 5C* primers. This is a direct comparison of anterior and posterior fat body *Dronc* expression. For both 10 and 12 hrs. APF, the results were attained by dividing the anterior fat body expression by the posterior fat body expression. This data consists only of samples for which the RNA OD260/280 ratio was greater than 1.5. When standard curve data was unavailable, an ideal primer efficiency of 2 was assumed. Standard error is expressed through error bars.

Using all samples with RNA OD260/280 ratios greater than 1.5, there was once again overexpression of *Dronc* in the posterior fat body cells. There was an anterior/posterior ratio of 0.694 for 10 hrs. APF, and 0.534 for 12 hrs. APF.

Table 14. All Data (regardless of OD260/280 value or lack of Tm measurement) *Dronc* Expression in the anterior fat body divided by that of the posterior fat body. This table shows the RT-qPCR expression ratios for each sample, using *Dronc* and *Actin 5C* primers. This is a direct comparison of anterior and posterior fat body *Dronc* expression. For both 10 and 12 hrs. APF, the results were attained by dividing the anterior fat body expression by the posterior fat body expression. Data is presented here regardless of RNA OD260/280 value, success in attaining a standard curve, or measurement of Tm. Samples for which the Tm was not measured are marked with an asterisk, like so*. When standard curve data was unavailable, an ideal primer efficiency of 2 was assumed. A value of 1 means that the anterior and posterior express *Dronc* equally, a value less than 1 indicates underexpression of *Dronc* in the anterior fat body, and a value greater than 1 indicates overexpression in the anterior fat body.

	10 hrs. APF anterior/posterior	12 hrs. APF anterior/posterior
10/27/2024-A1*	0.3371428571	0.5801033592
10/27/24-A2	1.346471127	0.5957792208
10/27/24-B1*	0.00796398892	0.588
3/3/25-A	0.4131283553	0.2528301887
10/27/24-B2		1.878522229
2/14/35-A	0.3236442516	0.8143835616
Average	0.4856701161	0.7849364266
Standard Deviation	0.5056571367	0.5650584182
Standard Error	0.2261367462	0.2306841332

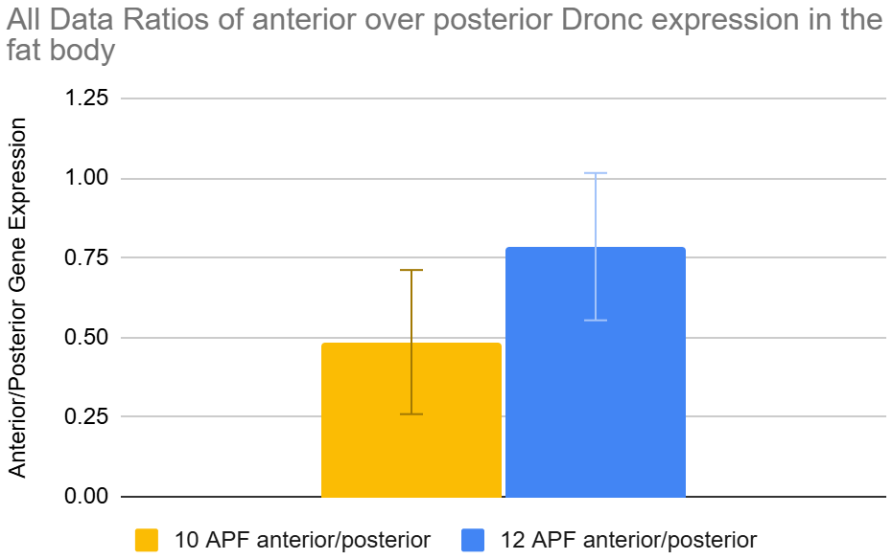

Figure 27. All Data (regardless of OD260/280 value or lack of Tm measurement) *Dronc* Expression in the anterior fat body divided by that of the posterior fat body, represented as a bar graph. This graph shows the RT-qPCR expression ratios for each sample, using *Dronc* and *Actin 5C* primers. This is a direct comparison of anterior and posterior fat body *Dronc* expression. For both 10 and 12 hrs. APF, the results were attained by dividing the anterior fat body expression by the posterior fat body expression. Data is presented here

regardless of RNA OD260/280 value, success in attaining a standard curve, or measurement of Tm. When standard curve data was unavailable, an ideal primer efficiency of 2 was assumed. Standard error is expressed through error bars.

Samples here were used regardless of RNA purity, standard curve, or lack of Tm measurements. This data should therefore be considered only when acknowledging its limitations. Despite the lower quality of samples included, this dataset follows the general trend. Both timepoints had overexpression of *Dronc* in the posterior fat body as compared to the anterior fat body. There was a higher degree of posterior overexpression at 10 hrs. APF, with a ratio of 0.486, and a lower degree of overexpression at 12 hrs. APF, with a ratio of 0.785.

Through consideration of each dataset, there seems to be a general trend of underexpression of *Dronc* in the anterior fat body, and overexpression of *Dronc* in the posterior fat body.

A one-sided t-test was performed to compare the mean anterior/posterior expression ratio to the theoretical expression ratio of 1. This was only possible for the 'All Data' dataset, due to low sample size. The mean anterior/posterior ratio at 10 hrs. APF ($M = 0.486$, $SD = 0.506$) was significantly different from the theoretical ratio of 1; $t(4) = -2.274$, $p = 0.043$. The mean anterior/posterior ratio at 12 hrs. APF ($M = 0.785$, $SD = 0.565$) was not significantly different from the theoretical ratio of 1; $t(5) = -0.932$, $p = 0.197$.

DISCUSSION

I. Observations of Dissections

Dissections were performed on Canton-S (CS) wild-type *Drosophila melanogaster*. In comparison to dissection of the 0 APF prepupae, at 10 and 12 hours APF, there was a noticeable increase in fat body remodeling. This effect was more pronounced in the 12 hrs. APF specimens than in those at 10 hrs. APF.

II. RNA Isolation Results Observations

Each RNA sample was analyzed by spectrophotometer, and determined to have high enough purity to process with cDNA synthesis. It should be noted that in previous investigation into *Dronc* expression (Cavale, 2023), the threshold for RNA purity was a OD260/280 ratio of 2 or higher. Throughout the course of this research, there was significant difficulty achieving a ratio of 2, and so a lower threshold of 1.5 was chosen. Due to a low number of samples with sufficient OD260/280 ratios, RNA samples with purities as low as 1.37 were also analyzed.

A possible contributor to the low RNA purity may have been the treatment of RNA samples with DNAse I before analysis. This idea is supported by the findings of Norhazlin et al. (2015). The research done by Cavale (2023) was performed without DNAse I treatment of RNA, and indicates no difficulty in attaining sufficient RNA purity.

III. RT-PCR and Gel Electrophoresis Results Observations

RT-PCR and gel electrophoresis were effective tools to determine primer efficiency. The DNA ladder worked well, allowing analysis of product size. Both

Dronc and *Actin 5C* primers resulted in a clear product at the appropriate base pair length in the gel. This proved that the primers were working as intended. The +RT positive control yielded bands, whereas the -RT (negative control) had only evidence of primer dimer, which was evidence of minimal contamination. Unlike RT-qPCR, there was no difficulty in achieving a product for the *Dronc* primer in gel electrophoresis.

IV. RT-qPCR Observations

A two-way ANOVA was performed to interpret the results of RT-qPCR. The 'Best Data' dataset had an insufficient sample size for analysis by ANOVA. The 'Best Data' dataset showed overexpression of *Dronc* in the posterior 10 hrs. APF fat body, as well as in both anterior and posterior 12 hrs. APF fat body. Underexpression of *Dronc* was observed only in the anterior 10 hrs. APF fat body. As analysis progresses through datasets (and the samples used become less reliable), each variable draws nearer to an average close to 1, with a notable exception. For each dataset, the average *Dronc* expression ratio for the posterior 10 hrs. APF fat body is greater than 2. Therefore, if there is a difference in *Dronc* expression between anterior and posterior tissues, it would be expected to be most noticeable at the 10 hrs. APF timepoint.

'RNA>1.5' had no significant evidence of difference between *Dronc* expression at 10 and 12 hrs. APF ($p=0.142$), and no significant evidence of difference between the anterior and posterior fat body cells ($p=0.186$). There was also no significant evidence of whether *Dronc* expression at 10 or 12 hrs. APF is

affected by the position of the fat body cells (p=0.571). ‘All Data’, a dataset composed of all samples regardless of RNA OD260/280 ratio, standard curve, or Tm measurements, was also analyzed by ANOVA. Here, there was once again no significant difference between *Dronc* expression at 10 and 12 hrs. APF (p=0.235), and no significant evidence of difference between the anterior and posterior fat body cells (p=0.193). While there was no significant evidence of whether *Dronc* expression at 10 or 12 hrs. APF is affected by the position of the fat body cells (p=0.15), the p-value for this combined variable was lower than for either APF or fat body position.

There was no significant difference in *Dronc* expression of the fat body between 10 and 12 hrs. APF. The initial hypothesis that *Dronc* would be underexpressed in the fat body at 10 hrs. APF could not be supported, due to the trend of underexpression in the anterior 10 hrs. APF fat body, and overexpression in the posterior 10 hrs. APF fat body.

The high variability in Cq between RT-qPCR runs presented a unique obstacle in comparing the anterior and posterior *Dronc* levels. Normalization of the fat body data was achieved by dividing the ΔΔCq of the anterior tissue by the ΔΔCq of its respective posterior tissue. This was done as a way to continue the precedent set by the math of the ΔΔCq method. The goal of ΔΔCq analysis is to know the expression of a gene of interest relative to a reference gene, and then use that value to compare the expression in a tissue of interest to a control tissue. This method results in a value that can be easily interpreted, with less than one being

underexpression, greater than one being overexpression, and one being equal expression in both samples. If the assumption of Cavale (2023) is correct, and there is no difference in *Dronc* expression between anterior and posterior adipocytes, then the ΔΔCq of the anterior value divided by the ΔΔCq of the posterior value should be equal to one. This analytic method was chosen, as opposed to determining the ΔCq of the anterior to that of the posterior, due to its inclusion of the salivary gland data. The ΔΔCq only provides an expression of one tissue or gene, relative to another. By comparing both values of ΔΔCq from anterior and posterior, this retains the data concerning the relative expression of each fat body sample to the salivary glands. This retains the insight provided by the salivary gland data, as well as allowing direct comparison.

It was only possible to test for significance with the 'All Data' dataset, due to the fact that each datapoint required an equivalent anterior and posterior sample. A one-sided t-test was performed, comparing the mean value against the theoretical equal ratio of 1. The mean anterior/posterior ratio at 10 hrs. APF (M = 0.486, SD = 0.506) was significantly different from the theoretical ratio of 1; $t(4) = -2.274$, $p = 0.043$. The mean anterior/posterior ratio at 12 hrs. APF (M = 0.785, SD = 0.565) was not significantly different from the theoretical ratio of 1; $t(5) = -0.932$, $p = 0.197$. While the results for 10 hrs. APF were significant, it is important to remember that this dataset used values which had sub-par OD260/280 ratios, unmeasured Tm values, or lacked a standard curve. As such, although this data is intriguing, it should not be taken as completely reliable.

V. Implications and Interpretations of RT-qPCR Results

Although the primary goal of this research was to increase the dataset from the research of Cavale (2023), it was not possible to analyze these results in combination with Cavale's. This is attributed not only to the differences in procedure, but also to the inherent variability of the results. Cavale (2023) did not include a DNase-I step for RNA purification. While DNase-I treatments can remove excess DNA from an RNA sample, it also decreases the RNA OD 260/280 ratios (Norhazlin et al., 2015). Therefore, it is unsurprising that RNA OD260/280 ratios for these experiments were lower than the ideal value of 2, which Cavale (2023) used as a minimum value. Furthermore, Cavale (2023) did not differentiate between anterior and posterior fat body cells, and so it was not possible to include those results in the ANOVA. Cavale (2023) observed underexpression of *Dronc* in the fat body at both 10 and 12 hrs. APF, though the sample size was too small to test for significance. Similar trends were found by Daish et al. (2004).

In my research, such a trend of underexpression was only observed for the anterior fat body tissues. It is not surprising that there was less of a difference between the 12 hrs. APF fat body *Dronc* expression, for both anterior and posterior tissues. This is likely due to the fact that ecdysone could have already had time to be processed by the fat bodies or salivary glands. PCD is a highly controlled process, with several activators as well as inhibitors. It is entirely possible that the decrease in *Dronc* expression of the 12 hrs. APF fat body is due

to degradation by these inhibitors after a longer period of time than the 10 hrs. APF fat body was exposed to.

The hypothesis that there would be more *Dronc* expression in the anterior fat body than in the posterior was not supported for 10 hrs. APF. The 12 hrs. APF data followed a similar trend, but the results were not significant. This directly contradicts the hypothesis that physical proximity to the ring gland (the source of ecdysone) could be positively correlated with a higher *Dronc* expression in the fat body. At this time, the exact reason behind this pattern remains unclear.

A potential influence on the *Dronc* overexpression in posterior fat body cells is the PCD known to occur in the midgut in the early prepupal phase (Jiang et al., 1997). These fat body cells are closer to the end deemed ‘posterior’, and thus would have been in closer proximity to the midgut than those ‘anterior’. Cell death of the larval midgut occurs at an earlier phase in prepupal development, and before salivary gland PCD takes place. Midgut cell death is a response to exposure to a high titer of ecdysone, and during this cell death there is a high level of caspase activity (Denton et al., 2010). Salivary gland cell death is induced by a second, less intense pulse of ecdysone, which occurs around 12 hrs. APF, whereas the larval midgut cell death is induced at pupariation, 0 APF. Therefore, it is possible that the posterior fat body cells were exposed to a high concentration of ecdysone due to their physical proximity to the site of ecdysone release. This hypothesis is not without the caveat that larval midgut cell death can occur in *Dronc*-deficient prepupae. Larval midgut cell death occurs through a complex

combination of mechanisms, and is thought to rely primarily on autophagy. As such, although caspase activity is considered to be a normal part of midgut cell death, it should not be taken as proof that these caspases are influencing apoptosis of the fat body.

There is no significant mixing of anterior and posterior fat body tissues during dissociation (Nelliot et al., 2006), and so it is unlikely that the observed anterior/posterior ratios are a result of accidental misclassification of anterior and posterior tissues during dissection. However, this possibility cannot be ruled out. As such, any further research would necessitate the development of a more finely-tuned dissection technique.

It is possible that the posterior fat body overexpression of *Dronc* is influenced by the Dronc repressor DIAP1. The protein DIAP1 will bind to the prodomain of the caspase Dronc, thereby inhibiting its activity and further activation of the apoptotic pathway (Meier et al., 2000). It is important to distinguish that DIAP1 binds to preexisting Dronc proteins to repress caspase activity, rather than inhibiting transcription of Dronc entirely. Therefore, activation of DIAP1 in the posterior fat body cells could allow the observed *Dronc* overexpression, while preventing precocious cell death. With an RT-qPCR experiment, only mRNA levels of the gene of interest are quantified. For a gene such as *Dronc*, this means that an RT-qPCR experiment would provide data only on the amount of *Dronc* transcribed, as opposed to the amount of active Dronc proteins. In order to properly assess the role of DIAP1 and Dronc in apoptosis,

additional RT-qPCR should be run with *DIAP1* primers, as well as a Western Blot to determine protein synthesis levels.

VI. Experimental Errors

The most significant errors of this experiment were the low OD260/280 RNA sample ratios. Although the usual accepted threshold for OD260/280 ratios is 2.0 or higher (as was used by Cavale), these values were unattainable. As such, a minimum value of 1.5 was arbitrarily selected. The low RNA values were likely due to both inexperience with the technique, as well as the inherent OD260/280 ratio limitations imposed by the application of DNase-I (Norhazlin et al., 2015). As my own understanding of proper RNA extraction techniques improved, so too did the OD260/280 ratios. However, there was insufficient data from samples with ratios greater than 1.5. As a result, RT-qPCR proceeded with sub-par samples, in order to use the data that was available.

A less easily explained obstacle in the research was the lack of *Dronc* primer transcription in RT-qPCR. This took a considerable amount of time to identify, since there was no similar failure of *Dronc* transcription in the gel electrophoresis PCR. The *Dronc* primers used in this experiment were inherited from the research of Cavale (2023), so age was suspected to be a factor. Mixing another working dilution of the existing primers yielded no positive results. When new primers were ordered (from the same manufacturer as those used by Cavale), RT-qPCR transcription of *Dronc* was successful. A working dilution was used, as before. After the worker dilutions of primers had been thawed for use more than

ten times, there would be a sharp decrease in measured *Dronc* transcription, or no measured transcription at all. This number of ten uses before primer failure is not an exact figure, but rather an estimate from my experience with these reagents. When a new working dilution was prepared, *Dronc* transcription was once again successful. From these results, it seems reasonable to conclude that repeated thawing and refreezing of *Dronc* primers negatively affected ability to detect transcription via RT-qPCR. There was no such issue with the *Actin 5C* primers, which indicates that the *Dronc* primers may be more susceptible to degradation.

When the *Dronc* primers failed, it was usually a complete failure to measure transcription. However, there were some occasions where such failure was preceded by an RT-qPCR run with dramatically decreased *Dronc* transcription. These results were excluded from analysis, because without a standard curve there was no way to determine the true amount of *Dronc* transcribed. Due to a lack of standard curve, the results from much of this research are unreliable. These results are only pulled further into question, in combination with the possibility of *Dronc* primer failure at a label not detectable without standard curve.

Another significant error was my own lack of familiarity with RT-qPCR protocol. This is why very few samples have available standard curve data, because I was improperly mixing the standard curve reagents. Furthermore, each sample should have been performed in triplicate, rather than duplicate as was done here. This was done in effort not to waste reagents during the

aforementioned struggle with *Dronc* primers. After the issue with primers was resolved, I neglected to amend the plate layout for running the experiment in triplicate. Due to a lack of triplicate technical replicates, the results are pulled further into question. The accuracy of data can be assessed through technical replicates, and so it is possible that this dataset includes statistical outliers that would have otherwise been identified.

VII. Conclusion and Future Directions

To conclude, the primary hypothesis was that larval salivary gland cells undergoing apoptosis would overexpress *Dronc*, as was found by Cavale (2023). The data does not support this hypothesis, showing a trend of overexpression of *Dronc* in the fat body, as compared to the salivary gland. It is worth noting that although Cavale measured underexpression of *Dronc* in the fat body, the sample sizes were 1 and 2 for 10 and 12 hrs. APF, respectively. The sample sizes in this study are larger, but with the caveat that most of this data lacks a standard curve, and that Cavale only used RNA with an OD260/280 ratio of 2 or greater. In sum, the data collected contradicts the hypothesis, but lacks the significance necessary to disprove it.

The secondary hypothesis was that in prepupae, anteriorly positioned fat body cells would have a higher *Dronc* expression than fat body cells positioned posterior. The data collected refute this hypothesis, showing consistent overexpression of *Dronc* in the posterior fat body as opposed to the anterior. It was only possible to do statistical analysis with the ‘All Data’ dataset here, but a

one-sided t-test showed significant difference between the 10 hrs. APF anterior/posterior *Dronc* ratio and the theoretical ratio of 1. Despite a lack of reliable results, the overall trend of anterior underexpression is consistent between datasets.

Further research is needed to determine the true role of *Dronc* in salivary gland apoptosis, as well as how the spread of ecdysone influences fat body cell fate. Despite the inherent flaws of this research, the trends it presents are still worthy of further exploration. It was predicted that the salivary glands would have overexpression of *Dronc*, but it was the posterior fat body at 10 hrs. APF that had the highest overexpression of *Dronc*. The variability between anterior and posterior fat body *Dronc* expression calls into question the use of the fat body as a control tissue. The fat body was selected as a control due to its non-lethal response to ecdysone, the same hormone which induces apoptosis in the salivary glands. It was consistently shown that there was relative underexpression of *Dronc* in the anterior fat body, as opposed to the posterior. There is little research on the differences in gene expression for adipose tissue in different parts of the larvae. Therefore, any use of the fat body as a control tissue should proceed with caution. If one were to exclusively use anterior fat body tissue for this experiment, then there would appear to be a trend of *Dronc* underexpression in the fat body, as predicted. Past research has made no distinction between anterior and posterior fat body tissue. By exclusively using anterior adipocytes, it would therefore be possible to influence results to support the hypothesis, in a way that would be

relatively undetectable. This would pose a massive issue for scientific replicability, since a relatively innocuous difference in dissections could impact gene expression so dramatically.

The first step for any further research would be to develop a new dissection technique. The techniques in this research were rudimentary, and so the classifications of anterior and posterior are less than perfect. Ideally, this new dissection method could include removal of adipocytes from each larval organ which they contact, such as salivary glands and midgut. This would provide a more comprehensive understanding of different tissue responses to increased ecdysone titer.

Yet another necessity for further research would be stricter regulations on which data must be excluded. RNA OD260/280 ratios should be 2 or greater for each sample, but this was difficult to achieve. A ratio below 2 indicated low RNA concentration in the sample. I attributed the low OD260/280 ratios to the use of DNase-I for purification. Therefore, any further testing should omit the DNase-I treatment, and only proceed if the OD260/280 ratio is 2 or greater. Another issue in regards to subpar data would be the inclusion of RT-qPCR values for samples which lacked a corresponding standard curve. The standard curve is essential, to ensure that gene expression is being correctly quantified. Future research would ideally only include datapoints which have corresponding standard curves.

Finally, there are additions to be made to the procedure. There should be additional RT-qPCR performed with *DIAP1* primers, as well as Western Blots for

both Dronc and DIAP1. RT-qPCR with *DIAP1* primers was originally a goal of Cavale (2023), however transcription with these primers was unsuccessful. Future research into this topic should include *DIAP1* RT-qPCR, perhaps with primers ordered from a new manufacturer. It's also possible that the *DIAP1* primers were susceptible to degradation over time, much like the Dronc primers. Therefore, a fresh working dilution of these primers should be maintained. Through quantification of *DIAP1* transcription, the repressor of *Dronc*, one would achieve a better understanding of why tissues not experiencing apoptosis could have high *Dronc* transcription rates. It should not be assumed that the *DIAP1* primers will work for RT-qPCR. Therefore, it would be also reasonable to perform DIAP1 and Dronc Western Blots. These Western Blots would provide information about the individual protein levels in each tissue. Posterior adipocytes exhibited *Dronc* overexpression, but did not appear to experience apoptosis. If there were also upregulation of *DIAP1* at this time, then it would explain why *Dronc* overexpression here was not correlated with apoptosis. A lack of active Dronc protein detected by Western Blot would support this hypothesis.

In conclusion, while the data did not support the hypothesis, it illustrated interesting trends worthy of further analysis. Particularly of interest are the posterior fat body cells, which expressed an unexpectedly high level of *Dronc* overexpression. Regardless, both anterior and posterior adipocyte caspase expression patterns should be explored.

WORKS CITED

Adams, G. (2020). A beginner's guide to RT-PCR, qPCR and RT-qPCR. *The Biochemist*, *42*(3), 48–53. https://doi.org/10.1042/BIO20200034

Aguila, J. R., Suszko, J., Gibbs, A. G., & Hoshizaki, D. K. (2007). The role of larval fat cells in adult *Drosophila melanogaster*. *Journal of Experimental Biology*, *210*(6), 956–963. https://doi.org/10.1242/jeb.001586

Alocca, M., Zola, S., & Bellosta, P. (2018). The Fruit Fly, Drosophila melanogaster: The Making of a Model (Part I). In F. K. Perveen (Ed.), *Drosophila melanogaster—Model for Recent Advances in Genetics and Therapeutics*. InTech. https://doi.org/10.5772/intechopen.72832

Anson, F., Thayumanavan, S., & Hardy, J. A. (2021). Exogenous Introduction of Initiator and Executioner Caspases Results in Different Apoptotic Outcomes. *JACS Au*, *1*(8), 1240–1256. https://doi.org/10.1021/jacsau.1c00261

Baehrecke, E. H. (2000). Steroid regulation of programmed cell death during Drosophila development. *Cell Death & Differentiation*, *7*(11), 1057–1062. https://doi.org/10.1038/sj.cdd.4400753

Basumatary, D., & Deka, N. (2024). Comprehensive study on the life cycle, morphology, and culturing techniques of drosophila melanogaster in laboratory conditions. *International Journal of Entomology Research*, *9*(7), 148–150.

Beira, J. V., & Paro, R. (2016). The legacy of Drosophila imaginal discs. *Chromosoma*, *125*(4), 573–592. https://doi.org/10.1007/s00412-016-0595-4

Bond, N. D., Hoshizaki, D. K., & Gibbs, A. G. (2010). The role of 20-hydroxyecdysone signaling in Drosophila pupal metabolism. *Comparative Biochemistry and Physiology Part A: Molecular & Integrative Physiology*, *157*(4), 398–404. https://doi.org/10.1016/j.cbpa.2010.08.025

Bond, N. D., Nelliot, A., Bernardo, M. K., Ayerh, M. A., Gorski, K. A., Hoshizaki, D. K., & Woodard, C. T. (2011). ßFTZ-F1 and Matrix metalloproteinase 2 are required for fat-body remodeling in Drosophila. *Developmental Biology*, *360*(2), 286–296. https://doi.org/10.1016/j.ydbio.2011.09.015

Broadus, J., McCabe, J. R., Endrizzi, B., Thummel, C. S., & Woodard, C. T. (1999). The Drosophila βFTZ-F1 Orphan Nuclear Receptor Provides Competence for Stage-Specific Responses to the Steroid Hormone

Ecdysone. *Molecular Cell*, *3*(2), 143–149. https://doi.org/10.1016/S1097-2765(00)80305-6
Cavale, S. K. (2023). *Regulation of Programmed Cell Death by Diap1 and Dronc During Drosophila Metamorphosis.* Mount Holyoke College.
Cherbas, L., Lee, K., & Cherbas, P. (1991). Identification of ecdysone response elements by analysis of the Drosophila Eip28/29 gene. *Genes & Development*, *5*(1), 120–131. https://doi.org/10.1101/gad.5.1.120
Chmurska, A., Matczak, K., & Marczak, A. (2021). Two Faces of Autophagy in the Struggle against Cancer. *International Journal of Molecular Sciences*, *22*(6), 2981. https://doi.org/10.3390/ijms22062981
Colombani, J., Bianchini, L., Layalle, S., Pondeville, E., Dauphin-Villemant, C., Antoniewski, C., Carré, C., Noselli, S., & Léopold, P. (2005). Antagonistic Actions of Ecdysone and Insulins Determine Final Size in *Drosophila*. *Science*, *310*(5748), 667–670. https://doi.org/10.1126/science.1119432
Daish, T. J., Mills, K., & Kumar, S. (2004). Drosophila Caspase DRONC Is Required for Specific Developmental Cell Death Pathways and Stress-Induced Apoptosis. *Developmental Cell*, *7*(6), 909–915. https://doi.org/10.1016/j.devcel.2004.09.018
Denton, D., Shravage, B. V., Simin, R., Baehrecke, E. H., & Kumar, S. (2010). Larval midgut destruction in Drosophila: Not dependent on caspases but suppressed by the loss of autophagy. *Autophagy*, *6*(1), 163–165. https://doi.org/10.4161/auto.6.1.10601
Elmore, S. (2007b). Apoptosis: A Review of Programmed Cell Death. *Toxicologic Pathology*, *35*(4), 495–516. https://doi.org/10.1080/01926230701320337
Fernández-Moreno, M. A., Farr, C. L., Kaguni, L. S., & Garesse, R. (2007). Drosophila melanogaster as a model system to study mitochondrial biology. *Methods in Molecular Biology (Clifton, N.J.)*, *372*, 33–49. https://doi.org/10.1007/978-1-59745-365-3_3
Franz, A., Wood, W., & Martin, P. (2018). Fat Body Cells Are Motile and Actively Migrate to Wounds to Drive Repair and Prevent Infection. *Developmental Cell*, *44*(4), 460-470.e3. https://doi.org/10.1016/j.devcel.2018.01.026
Green, D. R. (2022a). Caspase Activation and Inhibition. *Cold Spring Harbor Perspectives in Biology*, *14*(8), a041020. https://doi.org/10.1101/cshperspect.a041020

Green, D. R. (2022b). Caspases and Their Substrates. *Cold Spring Harbor Perspectives in Biology*, *14*(3), a041012. https://doi.org/10.1101/cshperspect.a041012

Hay, B. A., & Guo, M. (2006). Caspase-Dependent Cell Death in *Drosophila*. *Annual Review of Cell and Developmental Biology*, *22*(1), 623–650. https://doi.org/10.1146/annurev.cellbio.21.012804.093845

Ho, J. (2014). The Regulation of Apoptosis in Kidney Development: Implications for Nephron Number and Pattern? *Frontiers in Pediatrics*, *2*. https://doi.org/10.3389/fped.2014.00128

Jiang, C., Baehrecke, E. H., & Thummel, C. S. (1997). Steroid regulated programmed cell death during *Drosophila* metamorphosis. *Development*, *124*(22), 4673–4683. https://doi.org/10.1242/dev.124.22.4673

Jindra, M., Palli, S. R., & Riddiford, L. M. (2013). The Juvenile Hormone Signaling Pathway in Insect Development. *Annual Review of Entomology*, *58*(1), 181–204. https://doi.org/10.1146/annurev-ento-120811-153700

Julien, O., & Wells, J. A. (2017). Caspases and their substrates. *Cell Death & Differentiation*, *24*(8), 1380–1389. https://doi.org/10.1038/cdd.2017.44

Khalid, N., & Azimpouran, M. (2025). Necrosis Pathology. In *StatPearls*. StatPearls Publishing. http://www.ncbi.nlm.nih.gov/books/NBK557627/

Kim, J. H., Shoemaker, A. M., Hutchings, K. A., Shinde, S., & Andrew, D. J. (2026). The Drosophila larval salivary gland, a simple and elegant model system to understand secretory organ development and function. *Current Opinion in Insect Science*, *73*, 101435. https://doi.org/10.1016/j.cois.2025.101435

Kornbluth, S., & White, K. (2005). Apoptosis in *Drosophila*: Neither fish nor fowl (nor man, nor worm). *Journal of Cell Science*, *118*(9), 1779–1787. https://doi.org/10.1242/jcs.02377

Lafont, R., Balducci, C., & Dinan, L. (2021). Ecdysteroids. *Encyclopedia*, *1*(4), 1267–1302. https://doi.org/10.3390/encyclopedia1040096

Lavorgna, G., Karim, F. D., Thummel, C. S., & Wu, C. (1993). Potential role for a FTZ-F1 steroid receptor superfamily member in the control of Drosophila metamorphosis. *Proceedings of the National Academy of Sciences*, *90*(7), 3004–3008. https://doi.org/10.1073/pnas.90.7.3004

Lee, C.-Y., Simon, C. R., Woodard, C. T., & Baehrecke, E. H. (2002). Genetic Mechanism for the Stage- and Tissue-Specific Regulation of Steroid Triggered Programmed Cell Death in Drosophila. *Developmental Biology*, *252*(1), 138–148. https://doi.org/10.1006/dbio.2002.0838

Liu, Y., Liu, H., Liu, S., Wang, S., Jiang, R., & Li, S. (2009). Hormonal and nutritional regulation of insect fat body development and function. *Archives of Insect Biochemistry and Physiology*, *71*(1), 16–30. https://doi.org/10.1002/arch.20290

Lopez, J., & Tait, S. W. G. (2015). Mitochondrial apoptosis: Killing cancer using the enemy within. *British Journal of Cancer*, *112*(6), 957–962. https://doi.org/10.1038/bjc.2015.85

Meier, P., Silke, J., Leevers, S. J., & Evan, G. I. (2000). The Drosophila caspase DRONC is regulated by DIAP1. *The EMBO Journal*, *19*(4), 598–611. https://doi.org/10.1093/emboj/19.4.598

Mustafa, M., Ahmad, R., Tantry, I. Q., Ahmad, W., Siddiqui, S., Alam, M., Abbas, K., Moinuddin, Hassan, Md. I., Habib, S., & Islam, S. (2024). Apoptosis: A Comprehensive Overview of Signaling Pathways, Morphological Changes, and Physiological Significance and Therapeutic Implications. *Cells*, *13*(22), 1838. https://doi.org/10.3390/cells13221838

Nelliot, A., Bond, N., & Hoshizaki, D. K. (2006). Fat-body remodeling in *Drosophila melanogaster*. *Genesis*, *44*(8), 396–400. https://doi.org/10.1002/dvg.20229

Norhazlin, J., Nor-Ashikin, M. N. K., Hoh, B. P., Sheikh Abdul Kadir, S. H., Norita, S., Mohd-Fazirul, M., Wan-Hafizah, W. J., Razif, D., Rajikin, M. H., & Abdullah, B. (2015). Effect of DNase treatment on RNA extraction from preimplantation murine embryos. *Genetics and Molecular Research*, *14*(3), 10172–10184. https://doi.org/10.4238/2015.August.28.1

Ouyang, L., Shi, Z., Zhao, S., Wang, F. -T., Zhou, T. -T., Liu, B., & Bao, J. -K. (2012). Programmed cell death pathways in cancer: A review of apoptosis, autophagy and programmed necrosis. *Cell Proliferation*, *45*(6), 487–498. https://doi.org/10.1111/j.1365-2184.2012.00845.x

Pfaffl, M. W. (2001). A new mathematical model for relative quantification in real-time RT-PCR. *Nucleic Acids Research*, *29*(9), 45e–445. https://doi.org/10.1093/nar/29.9.e45

Riddiford, L. M. (1993). Hormone receptors and the regulation of insect metamorphosis. *Receptor*, *3*(3), 203–209.

Schubiger, M., Carré, C., Antoniewski, C., & Truman, J. W. (2005). Ligand-dependent de-repression via EcR/USP acts as a gate to coordinate the differentiation of sensory neurons in the *Drosophila* wing. *Development*, *132*(23), 5239–5248. https://doi.org/10.1242/dev.02093

Sharma, V. K., Singh, T. G., Singh, S., Garg, N., & Dhiman, S. (2021). Apoptotic Pathways and Alzheimer's Disease: Probing Therapeutic

Potential. *Neurochemical Research*, *46*(12), 3103–3122. https://doi.org/10.1007/s11064-021-03418-7

Shen, S., Shao, Y., & Li, C. (2023). Different types of cell death and their shift in shaping disease. *Cell Death Discovery*, *9*(1), 284. https://doi.org/10.1038/s41420-023-01581-0

Woodard, C. T., Baehrecke, E. H., & Thummel, C. S. (1994). A molecular mechanism for the stage specificity of the Drosophila prepupal genetic response to ecdysone. *Cell*, *79*(4), 607–615. https://doi.org/10.1016/0092-8674(94)90546-0

Yamanaka, N., Rewitz, K. F., & O'Connor, M. B. (2013). Ecdysone control of developmental transitions: Lessons from Drosophila research. *Annual Review of Entomology*, *58*, 497–516. https://doi.org/10.1146/annurev-ento-120811-153608

APPENDIX 1

Below are the Cq values from individual RT-qPCR runs, with the corresponding calculations done to determine the gene expression ratio. The top left corner of each table indicates the identity of the samples. The top row represents the gene primer used, the tissue type, and hours APF. It should be read as follows: X-YY-ZZ. X indicates if the primer was either A for *Actin 5C* or D for *Dronc*. YY represents SG (salivary glands), aFB (anterior fat body), or pFB (posterior fat body). ZZ indicates whether the sample was collected at 10 or 12 hours APF. Samples with a melting temperature (Tm) of less than 80℃ were excluded from Best Data/RNA> 1.5, and so it was only recorded whether the Tm was less than or greater than 80℃. Rows marked as having a Tm>80℃ had this measurement for both replicates 1 and 2. When the instrument failed to measure Tm, the recorded value was ‘none’.

Appendix 1.1

10/27/24 A1	A-SG-10	A-aFB-10	A-pFB-10	D-SG-10	D-aFB-10	D-pFB-10	A-SG-12	A-aFB-12	A-pFB-12	D-SG-12	D-aFB-12	D-pFB-12
Replicate 1 Cq	29.64	17.16	18.53	34.85	26.75	26.9	20.3	18.79	18	27.22	26.91	24.97
Replicate 2 Cq	29.58	16.92	18.81	35.64	26.77	26.74	20.26	18.48	17.97	27.3	26.63	25.7
average Cq	29.61	17.04	18.67	35.245	26.76	26.82	20.28	18.635	17.985	27.26	26.77	25.335
%CV= (standev/mean)*100	0.14328404 89	0.995925 0439	1.060 47080 2	1.58 4946 396	0.052 8480 4045	0.421 83849 74	0.13 9468 7931	1.17 6297 838	0.117 9494 214	0.20 7514 8294	0.739 59618 5	2.03 7449 971
subtract average A from correlating average D				5.635	9.72	8.15				6.98	8.135	7.35
subtract sg from fb value					4.085	2.515					1.155	0.37
efficiency^(-[value])= Expression Ratio					0.058 9240 3349	0.174 94823 32					0.449 06618 64	0.77 3782 4968
Tm	none	none	none	none	none	none	none	none	none	none	none	none

Appendix 1.2

10/27/24 A2	A-SG-10	A-aFB-10	A-pFB-10	D-SG-10	D-aFB-10	D-pFB-10	A-SG-12	A-aFB-12	A-pFB-12	D-SG-12	D-aFB-12	D-pFB-12
Replicate 1 Cq	18.21	18.86	18.26	28.05	28.71	27.77	21.59	17.12	19.31	29.18	26.55	28.2
Replicate 2 Cq	18.27	19.22	17.91	none	27.88	none	21.61	17.22	19.72	29.98	26.64	28.19
average Cq	18.24	19.04	18.085	28.05	28.295	27.77	21.6	17.17	19.515	29.58	26.595	28.195
%CV =(standev/mean)*100	0.232600 9149	1.336 966603	1.36 8467 644	none	2.074 21321 2	none	0.065472 85011	0.411 8268 964	1.485 59457	1.91 2391 565	0.239 29163 49	0.025 0791 5521
subtract average A from correlating average D				9.81	9.255	9.685				7.98	9.425	8.68
subtract sg from fb value					-0.555	-0.125					1.445	0.7
efficiency^(-[value])= Expression Ratio					1.469 168633	1.090 507733					0.367 292158 3	0.615 5722 067
Tm	>80	>80	>80	>80	>80	>80	>80	>80	>80	>80	>80	>80

Appendix 1.3

10/27/24 B1	A-SG-10	A-aFB-10	A-pFB-10	D-SG-10	D-aFB-10	D-pFB-10	A-SG-12	A-aFB-12	A-pFB-12	D-SG-12	D-aFB-12	D-pFB-12
Replicate 1 Cq	26.2	18.96	20.08	33.79	36.18	26.27	22.88	24.61	19.19	28.1	30.96	25.09
Replicate 2 Cq	26.46	18.65	19.68	none	27.23	25.35	22.71	24.29	19.56	27.26	30.07	24.26
average Cq	26.33	18.805	19.88	33.79	31.705	25.81	22.795	24.45	19.375	27.68	30.515	24.675
%CV =(standev/mean)*100	0.698244478	1.165663931	1.422750063	none	19.960907 4	2.520489108	0.527344 3861	0.925456 7279	1.350345853	2.145844278	2.062346503	2.378515211
subtract average A from correlating average D				7.46	12.9	5.93				4.885	6.065	5.3
subtract sg from fb value					5.44	-1.53					1.18	0.415
efficiency^(-[value])= Expression Ratio					0.023035456 52	2.887858391					0.441351498 1	0.750019 4946
Tm	none	none	none	none	none	none	none	none	none	none	none	none

Appendix 1.4

10/27/24 B2	A-SG-10	A-aFB-10	A-pFB-10	D-SG-10	D-aFB-10	D-pFB-10	A-SG-12	A-aFB-12	A-pFB-12	D-SG-12	D-aFB-12	D-pFB-12
Replicate 1 Cq							23.17	25.67	20.01	35.36	35.32	29.72
Replicate 2 Cq							22.98	25.76	19.57	32.48	34.63	30.2
average Cq							23.075	25.715	19.79	33.92	34.975	29.96
%CV =(standev/mean)*100							0.58223310 26	0.247 4804 99	1.57 2142 414	6.00 3736 821	1.39 5006 945	1.132 88135 8
subtract average A from correlating average D										10.845	9.26	10.17
subtract sg from fb value											-1.585	-0.675
efficiency^(-[value])= Expression Ratio											5.41 7467 271	2.053 52502 6
Tm	>80	>80	>80	>80	>80	>80	>80	>80	>80	>80	>80	>80

Appendix 1.5

2/14/25 A	A-SG-10	A-aFB-10	A-pFB-10	D-SG-10	D-aFB-10	D-pFB-10	A-SG-12	A-aFB-12	A-pFB-12	D-SG-12	D-aFB-12	D-pFB-12
Replicate 1 Cq	21.06	18.79	19.75	27.83	26.23	24.9	21.77	17.17	18.46	27.88	23.5	23.54
Replicate 2 Cq	21.5	19.61	20.21	26.96	25.42	25.07	21.62	17.4	17.67	28.05	23.54	24.41
average Cq	21.28	19.2	19.98	27.395	25.825	24.985	21.695	17.285	18.065	27.965	23.52	23.975
%CV= (standev/mean)*100	1.462062893	3.019935211	1.6279735 7	2.245602846	2.217837339	0.481121284	0.488896138 2	0.940899969 2	3.092246649	0.42985214 66	0.120256255 3	2.565934931
subtract average A from correlating average D				6.115	6.625	5.005				6.27	6.235	5.91
subtract sg from fb value					0.51	-1.11					-0.035	-0.36
efficiency^(-[value])= Expression Ratio					0.702222 4379	2.158456473					1.024556 823	1.283425898
Tm	>80	>80	>80	>80	>80	>80	>80	>80	>80	>80	>80	>80

Appendix 1.6

3/3/25 A	A-SG-10	A-aFB-10	A-pFB-10	D-SG-10	D-aFB-10	D-pFB-10	A-SG-12	A-aFB-12	A-pFB-12	D-SG-12	D-aFB-12	D-pFB-12
Replicate 1 Cq	27.53	24.74	27.53	33.43	30.13	30.62	22.14	18.39	18.18	24.23	24.43	22.02
Replicate 2 Cq	27.92	25.13	27.38	34.01	30.21	32.2	22.22	18.51	18.08	24.13	24.28	22.07
average Cq	27.725	24.935	27.455	33.72	30.17	31.415	22.18	18.45	18.13	24.18	24.355	22.045
%CV= (standev/mean)*100	0.994667 7896	1.1059620 8	0.3863267 79	1.21625 7216	0.18749 93122	3.53384 5763	0.25504 3023	0.45990 68496	0.39002 02875	0.29243 45662	0.43549 99679	0.16037 80406
subtract average A from correlating average D				5.995	5.235	3.96				2	5.905	3.915
subtract sg from fb value					-0.76	-2.035					3.905	1.915
efficiency^(-[value])= Expression Ratio					1.693490 625	4.098227 292					0.066754 088	0.265171 9353
Tm	>80	>80	>80	>80	>80	>80	>80	>80	>80	>80	>80	>80

Appendix 2

Below are the OD260/280 ratios of each sample. The tissue column is written as follows: S (salivary glands), aFB (anterior fat body), or pFB (posterior fat body). The APF column indicates whether the sample was collected at 10 or 12 hours APF.

Appendix 2.1

Collection Date	Tissue	APF	OD260/280
10/27-A1	S	10	1.65
10/27-A1	aFB	10	1.56
10/27-A1	pFB	10	1.87
10/27-A1	S	12	1.46
10/27-A1	aFB	12	1.65
10/27-A1	pFB	12	1.64

Appendix 2.2

Collection Date	Tissue	APF	OD260/280
10/27-A2	S	10	1.65
10/27-A2	aFB	10	1.56
10/27-A2	pFB	10	1.87
10/27-A2	S	12	1.46
10/27-A2	aFB	12	1.65
10/27-A2	pFB	12	1.64

Appendix 2.3

Collection Date	Tissue	APF	OD260/280
10/27-B1	S	10	1.37
10/27-B1	aFB	10	1.56
10/27-B1	pFB	10	1.77
10/27-B1	S	12	1.55
10/27-B1	aFB	12	1.47
10/27-B1	pFB	12	1.6

Appendix 2.4

Collection Date	Tissue	APF	OD260/280
10/27-B2	S	10	1.37
10/27-B2	aFB	10	1.56
10/27-B2	pFB	10	1.77
10/27-B2	S	12	1.55
10/27-B2	aFB	12	1.47
10/27-B2	pFB	12	1.6

Appendix 2.5

Appendix 2.6

Collection Date	Tissue	APF	OD260/280
2/14-A	S	10	1.4
2/14-A	aFB	10	1.53
2/14-A	pFB	10	1.57
2/14-A	S	12	1.47
2/14-A	aFB	12	1.57
2/14-A	pFB	12	1.59
3/3- A	S	10	1.89
3/3- A	aFB	10	1.76
3/3- A	pFB	10	1.83
3/3- A	S	12	1.58
3/3- A	aFB	12	1.69
3/3- A	pFB	12	1.69